PH4 of petunia is an R2R3-MYB protein that activates vacuolar acidification through interactions with Basic-Helix-Loop-Helix transcription factors of the anthocyanin pathway

Quattrocchio, F.M.; Verweij, C.W.; Kroon, A.R.; Spelt, C.E.; Mol, J.N.M.; Koes, R.E.

published in
The Plant Cell
2006

DOI (link to publisher)
10.1105/tpc.105.034041

document version
Publisher's PDF, also known as Version of record

The Plant Cell, Vol. 18, 1274–1291, May 2006, www.plantcell.org

PH4 of Petunia Is an R2R3 MYB Protein That Activates Vacuolar Acidification through Interactions with Basic-Helix-Loop-Helix Transcription Factors of the Anthocyanin Pathway[W]

Francesca Quattrocchio,[1] Walter Verweij,[1] Arthur Kroon, Cornelis Spelt, Joseph Mol, and Ronald Koes[2]

Institute for Molecular and Cellular Biology, Vrije Universiteit, 1081 HV Amsterdam, The Netherlands

The *Petunia hybrida* genes *ANTHOCYANIN1* (*AN1*) and *AN2* encode transcription factors with a basic-helix-loop-helix (BHLH) and a MYB domain, respectively, that are required for anthocyanin synthesis and acidification of the vacuole in petal cells. Mutation of *PH4* results in a bluer flower color, increased pH of petal extracts, and, in certain genetic backgrounds, the disappearance of anthocyanins and fading of the flower color. *PH4* encodes a MYB domain protein that is expressed in the petal epidermis and that can interact, like AN2, with AN1 and the related BHLH protein JAF13 in yeast two-hybrid assays. Mutation of *PH4* has little or no effect on the expression of structural anthocyanin genes but strongly downregulates the expression of *CAC16.5*, encoding a protease-like protein of unknown biological function. Constitutive expression of *PH4* and *AN1* in transgenic plants is sufficient to activate *CAC16.5* ectopically. Together with the previous finding that AN1 domains required for anthocyanin synthesis and vacuolar acidification can be partially separated, this suggests that AN1 activates different pathways through interactions with distinct MYB proteins.

INTRODUCTION

In plants, the vacuole occupies a large part (up to 90%) of the cell volume and is important for a variety of physiological processes, such as pH homeostasis, osmoregulation, ion transport, and storage of metabolites. Moreover, it plays an important role in cell growth, because the enlargement of a cell is mostly attributable to an increase in the volume of the vacuole rather than of the cytoplasm (reviewed in Taiz, 1992; Maeshima, 2001; Gaxiola et al., 2002).

The lumen of vacuoles is acidic compared with the cytoplasm, and in some cells (e.g., in lemon [*Citrus limon*] fruit) it can reach pH values as low as 1. Among the most abundant proteins on the vacuolar membrane are vacuolar ATPase (v-ATPase) and pyrophosphatase proton pumps (Szponarski et al., 2004) that transport protons from the cytoplasm into the vacuole, thereby contributing to the acidification of the vacuolar lumen. The resulting electrochemical gradient across the vacuolar membrane is the driving force for the transport of a variety of compounds (ions, sugars) via secondary symport and antiport transporters and channels (reviewed in Taiz, 1992; Maeshima, 2001; Gaxiola et al., 2002).

In most species, the coloration of flowers and fruits results from the accumulation of flavonoid pigments (anthocyanins) in the vacuoles of (sub)epidermal cells. Because the absorption spectrum of anthocyanins depends on the pH of their environment (de Vlaming et al., 1983), the color of a tissue depends in part on the pH of the vacuolar lumen, thus making flower color a convenient and reliable reporter to monitor alterations in vacuolar pH (Yoshida et al., 1995, 2003)

In morning glory (*Ipomoea tricolor*) petals, the vacuolar pH is relatively low when the flower bud opens, resulting in a red color, but upon further maturation, the vacuolar pH increases and the petals acquire a strong blue color (Yoshida et al., 1995). This color change and the increase of vacuolar pH require a putative Na^+/H^+ exchanger encoded by the *PURPLE* gene (Fukada-Tanaka et al., 2000). Most likely, PURPLE transports sodium ions into and protons out of the vacuole, resulting in a less acidic vacuole and a bluer color.

Petunia hybrida flowers normally have a lower pH than *Ipomoea* flowers, and the color of wild-type flowers stays on the reddish (low pH) side of the color spectrum. By genetic analyses, seven loci (named *PH1* to *PH7*) have been identified that, when mutated, cause a more bluish flower color and an increase in the pH of crude petal extracts (Wiering, 1974; de Vlaming et al., 1983; van Houwelingen et al., 1998), suggesting that these genes are required for acidification of the vacuole (de Vlaming et al., 1983). Mutations in the genes *ANTHOCYANIN1* (*AN1*), *AN2*, and *AN11* cause, besides the loss of anthocyanin pigments, an increased pH of petal extracts. That this pH shift is at least in part attributable to an increased pH of the vacuolar lumen was evident from the bluish flower color specified by particular *an1* alleles (formerly known as *ph6*) that lost the capacity to activate the vacuolar acidification function but could still drive anthocyanin synthesis (Spelt et al., 2002).

[1] These authors contributed equally to this work.

[2] To whom correspondence should be addressed. E-mail ronald.koes@falw.vu.nl; fax 31-20-5987155.

The authors responsible for distribution of materials integral to the findings presented in this article in accordance with the policy described in the Instructions for Authors (www.plantcell.org) are: Francesca Quattrocchio (francesca.quattrocchio@falw.vu.nl) and Ronald Koes (ronald.koes@falw.vu.nl).

[W] Online version contains Web-only data.

Article, publication date, and citation information can be found at www.plantcell.org/cgi/doi/10.1105/tpc.105.034041.

AN1 and *AN11* are required for transcriptional activation of a subset of structural anthocyanin genes, encoding the enzymes of the pathway, in all pigmented tissues (Quattrocchio et al., 1993) and encode a basic-helix-loop-helix (BHLH) transcription factor and a WD40 protein, respectively (de Vetten et al., 1997; Spelt et al., 2000). AN2 encodes a MYB-type transcription factor whose function appears to be (partially) redundant, because it is expressed only in petals and not in other pigmented tissues (Quattrocchio et al., 1999). Moreover, even in the *an2* null mutant, pigmentation of the petals is reduced, but not fully blocked, and the pH shift in *an2* petal homogenates is smaller than that in *an1* or *an11* petals (Quattrocchio et al., 1993; Spelt et al., 2002). In addition, AN1 and AN11 play a role in the development of epidermal cells in the seed coat (Spelt et al., 2002).

The anthocyanin pathway has been shown to be activated by similar MYB, BHLH, and WD40 proteins in a wide variety of species, indicating that this function is well conserved (reviewed in Winkel-Shirley, 2001; Koes et al., 2005). Several studies revealed that these MYB, BHLH, and WD40 proteins could interact physically, indicating that they may operate in one transcription activation pathway and may activate their target genes as a (ternary) complex (Goff et al., 1992; Zhang et al., 2003; Baudry et al., 2004; Kroon, 2004; Zimmermann et al., 2004). Besides petunia, *Arabidopsis thaliana* is the only other species in which these activators are known to control multiple processes.

In *Arabidopsis*, the WD40 protein TRANSPARENT TESTA GLABRA1 (TTG1) (Walker et al., 1999) is required for the synthesis of anthocyanin and proanthocyanidin pigments, the production of seed mucilage, and the development of trichomes on stems and leaves (Koornneef, 1981), whereas in roots it suppresses the formation of root hairs in certain cells (Galway et al., 1994). During the regulation of anthocyanin synthesis, trichome development, and nonhair development in the root, TTG1 cooperates with two functionally equivalent BHLH proteins encoded by *GLABRA3* (*GL3*) and *ENHANCER OF GLABRA3* (*EGL3*) (Payne et al., 2000; Bernhardt et al., 2003; Ramsay et al., 2003; Zhang et al., 2003), whereas synthesis of proanthocyanidins in the seed coat depends on a distinct BHLH protein encoded by *TRANSPARENT TESTA8* (*TT8*) (Nesi et al., 2000). TTG1 and GL3/EGL3 or TT8 activate these distinct processes by associating with distinct MYB partners. During trichome development, they interact with R2R3 MYBs encoded by *GLABROUS1* (*GL1*) or *MYB23* (Oppenheimer et al., 1991; Kirik et al., 2001, 2005), and for the development of nonhair cells in the root they interact with a functionally equivalent MYB encoded by *WEREWOLF* (*WER*) (Lee and Schiefelbein, 2001), whereas for anthocyanin synthesis, their MYB partner is probably PRODUCTION OF ANTHOCYANIN PIGMENT1 (PAP1) or PAP2 (Borevitz et al., 2000; Baudry et al., 2004; Zimmermann et al., 2004).

The involvement of anthocyanin regulators in trichome and root hair development is seen only in *Arabidopsis* and not in other species for which regulatory anthocyanin mutants have been isolated, such as *Antirrhinum majus*, maize (*Zea mays*), or petunia. Nevertheless, RED (R) (BHLH) and PALE ALEURONE COLOR (PAC1) (WD40) from maize can restore the hair defects in *Arabidopsis ttg1* mutants (Lloyd et al., 1992; Carey et al., 2004), indicating that the functional diversification did not depend on alterations in these WD40 and BHLH proteins but on the divergence of their MYB partners and/or their downstream target genes. Whether these MYB, BHLH, and WD40 proteins also activate vacuolar acidification in species other than petunia is unclear.

To unravel the mechanisms and the biochemical pathways by which AN1, AN11, and AN2 control vacuolar pH, we set out to isolate the genetically defined *PH* loci by transposon-tagging strategies and the downstream structural genes by RNA profiling methods. Here, we describe the isolation and molecular characterization of *PH4*. We show that *PH4* is a member of the MYB family of transcription factors that is expressed in the petal epidermis and that can interact physically with AN1 and JAF13, a functionally related BHLH protein that can also drive anthocyanin synthesis (Quattrocchio et al., 1998). Because PH4 plays no apparent role in anthocyanin synthesis, we propose that AN1 activates anthocyanin synthesis and vacuolar acidification through interactions with distinct MYB proteins.

RESULTS

Mutations That Alter pH in Petals

The petunia line R27 contains functional alleles for all of the regulatory anthocyanin genes that color the petal (*AN1*, *AN2*, and *AN11*) but contains mutations in the structural genes *HYDROXYLATION AT FIVE* (*HF1*) and *HF2*, both encoding FLAVONOID 3′5′ HYDROXYLASE (Holton et al., 1993), and *RHAMNOSYLATION AT THREE* (*RT*), encoding ANTHOCYANIN RHAMNOSYLTRANSFERASE (Kroon et al., 1994); consequently, the major anthocyanins synthesized are cyanidin derivatives (de Vlaming et al., 1984; Wiering and de Vlaming, 1984) (Figure 1). In addition, R27 is mutant for *FLAVONOL* (*FL*), which strongly reduces flavonol synthesis (Figure 1) and increases the accumulation of cyanidin derivatives (de Vlaming et al., 1984; Wiering and de Vlaming, 1984) (Figure 1). Consequently, the flowers of R27 have a bright red color (Figure 2A). The lines W138 and W137 derive from R27 by *dTPH1* insertions in *AN1* and *AN11*, respectively (alleles *an1-W138* and *an11-W137*), and, consequently, bear white flowers with red or pink revertant spots (Doodeman et al., 1984a, 1984b) (Figure 2B).

Among progeny of W138 and W137, we found several new mutations affecting flower color (van Houwelingen et al., 1998; Spelt et al., 2002). In one class of mutants, the color of the *AN1* or *AN11* revertant spots (in an *an1-W138* or *an11-W137* background) (Figure 2C) or of the whole corolla (in an *AN1* or *AN11* germinal revertant) had changed from red to purplish (Figures 2D and 2E). Subsequent complementation analyses showed that these mutations represented new alleles of *PH2* (allele *ph2-A2414*), *PH3* (allele *ph3-V2068*), and *PH4* (alleles *ph4-V2166*, *ph4-B3021*, *ph4-X2052*, and *ph4-V2153*) (see Supplemental Table 1 online). Yet another unstable *ph4* allele (*ph4-X2377*) was recovered from the Syngenta breeding program in a family segregating 3:1 for wild types with red petals and mutants with purplish petals with an occasional revertant red spot.

The alleles *ph4-V2166*, *ph4-V2153*, *an1-W138*, *an1-W225*, and *an11-W134* all cause a similar increase in petal extract pH (Figure 2F) (Spelt et al., 2002). To determine at which stage *AN1*,

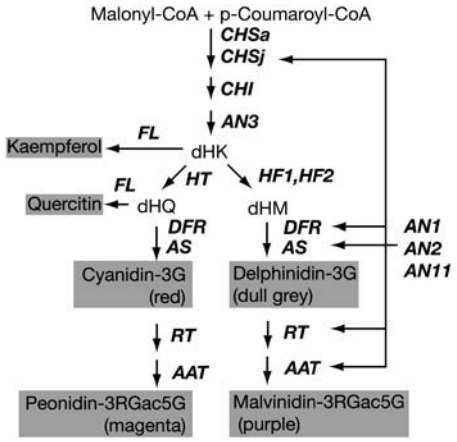

Figure 1. Genetic Control of the Anthocyanin Pathway in Petunia Petals.

The main anthocyanins and flavonols (gray boxes) are synthesized via a branched pathway. Genes that control distinct steps are indicated in boldface italics. Malonyl-CoA and *p*-coumaroyl-CoA are converted by the enzymes CHALCONE SYNTHASE (expressed from two distinct genes, *CHSa* and *CHSj*), CHALCONE ISOMERASE (encoded by *CHIa*), and FLAVONOID 3 HYDROXYLASE (encoded by *AN3*) into dihydrokaempferol (dHK). Hydroxylation of dHK on the 3′ or the 3′ plus 5′ position is controlled by *HT* (for *HYDROXYLATION AT THREE*) and the homologs *HF1* and *HF2* (for *HYDROXYLATION AT FIVE*) to yield dihydroquercitin (dHQ) and dihydromyricitin (dHM), respectively. The simplest anthocyanins in petunia flowers are 3-glucosides (3G). Through the action of *RT* (for *RHAMNOSYLATION AT FIVE*) and *AAT* (for *ANTHOCYANIN-RUTINOSIDE ACYLTRANSFERASE*) and others, anthocyanins with a 3-rutinoside *p*-coumaroyl-5-glucoside (3RGac5G) substitution pattern are generated. The colors displayed by the various anthocyanins (in a *fl PH* background) are shown in parentheses.

AN11, *PH3*, and *PH4* are active, we analyzed flowers of different developmental stages. Figure 2G shows that wild-type petals start to acidify around developmental stage 4, when the bud is about to open. In *an1*, *ph3*, and *ph4* mutants, this acidification is reduced but not blocked completely. This finding suggests that multiple vacuolar acidification pathways operate in petals, some of which are independent of *AN1*, *AN11*, *PH4*, and *PH3*. Analysis of double mutant flowers showed that the pH of *an1 ph4* or *an11 ph4* petal homogenates is not significantly different from that of any of the single mutants, suggesting that these genes operate in the same vacuolar acidification pathway (Figure 2F).

To test whether alterations in pigment synthesis also contributed to the color change in *ph4* petals, we analyzed anthocyanins in wild-type (R27) and *ph4-V2153* petals of closed buds (stage 4) by HPLC. Figure 2H shows that both genotypes accumulate a nearly identical mixture of anthocyanins. R27 petals synthesize only small amounts of flavonol copigments (quercetin derivatives) as a result of its *fl*/*fl* genotype, and HPLC analysis did not reveal clear differences in the accumulation of these compounds in *ph4* petals (see Supplemental Figure 1 online). Thus, the *ph4* mutation has, at least in the R27 genetic background, little or no effect on the synthesis and modification of anthocyanins.

Early genetic work had shown that a mutation in *PH4* or a closely linked gene triggers the complete fading of flower color and the disappearance of anthocyanins after opening of the flower bud, if combined with a dominant allele at the *FADING* locus (Wiering, 1974; de Vlaming et al., 1982). Anthocyanins with a 3RGac5G substitution pattern are particularly sensitive to fading, whereas the 3-glucosides (as in *rt* mutants like R27 and derived lines) and the 3-rutinosides show little or no fading (de Vlaming et al., 1982). When we crossed the unstable *ph4-V2166* allele into a genetic background that allows the synthesis of 3RGac5G-substituted anthocyanins, the flowers displayed upon opening a blue-violet color and were dotted with red-violet spots and sectors resulting from reversions of *ph4* (Figure 2H). In the next days, the color of the blue-violet (*ph4*) cells faded to nearly white, whereas the red-violet (*PH4*) revertant sectors retained their color. Control crosses with isogenic *PH4* plants (lines R27 and W138) yielded only progeny with evenly red-colored, nonfading corollas, whereas crosses with a stable recessive *ph4-V2153* parent gave only progeny with evenly colored blue-violet, fading corollas (*ph4*). This finding demonstrates that it is the mutation of *PH4*, and not that of a linked gene, that triggers fading.

The *an1-G621* allele expresses a truncated AN1 protein that can drive anthocyanin synthesis but not vacuolar acidification (Spelt et al., 2002). When crossed into a background that allows the synthesis of 3RGac5G-substituted anthocyanins, the *an1-G621* allele also triggered fading (Figure 2I), and similar results were obtained with the *an1-B3196* allele in distinct crosses.

Strikingly, the unstable *ph2-A2414* (Figure 2J) and *ph5* (data not shown) alleles did not induce fading when crossed into an *FA* background synthesizing 3RGAac5G-substituted anthocyanins, suggesting that fading in *an1* and *ph4* petals is not triggered by the upregulation of vacuolar pH alone and may depend on some other vacuolar defect.

Isolation of *PH4* Using Transposon-Tagged Alleles

Because most mutant alleles that arose in W138 were attributable to insertions of a 284-bp *dTPH1* transposon (Souer et al., 1996; de Vetten et al., 1997; van Houwelingen et al., 1998; Quattrocchio et al., 1999; Spelt et al., 2000; Tobeña-Santamaria et al., 2002; Vandenbussche et al., 2003), we anticipated that the unstable alleles *ph4-V2166*, *ph4-X2052*, and *ph4-B3021* might also harbor insertions of *dTPH1*.

To identify the *dTPH1* copy in *ph4-B3021*, we analyzed *dTPH1* flanking sequences in mutant and wild-type plants by transposon display (van den Broek et al., 1998) and found a 98-bp fragment that was amplified from the three *ph4-B3021* plants analyzed but not from the two wild-type plants homozygous for the parental PH4 allele (Figure 3A). Subsequent isolation, cloning, and sequencing of this fragment showed that it contained 66 bp of *dTPH1* sequence and 32 bp of flanking sequence that was identical to a cDNA clone (*MYBa*) that had been isolated independently by yeast two-hybrid screen using an AN1 bait (see below).

PCR experiments with gene-specific primers showed that in *ph4-B3021* and *ph4-V2166* plants, *MYBa* was disrupted by a 284-bp *dTPH1* insertion in the 5′ and 3′ ends of the protein-coding region, respectively (Figure 3B). Analysis of *PH4* progeny plants that originated from germinal reversions of *ph4-B3021*

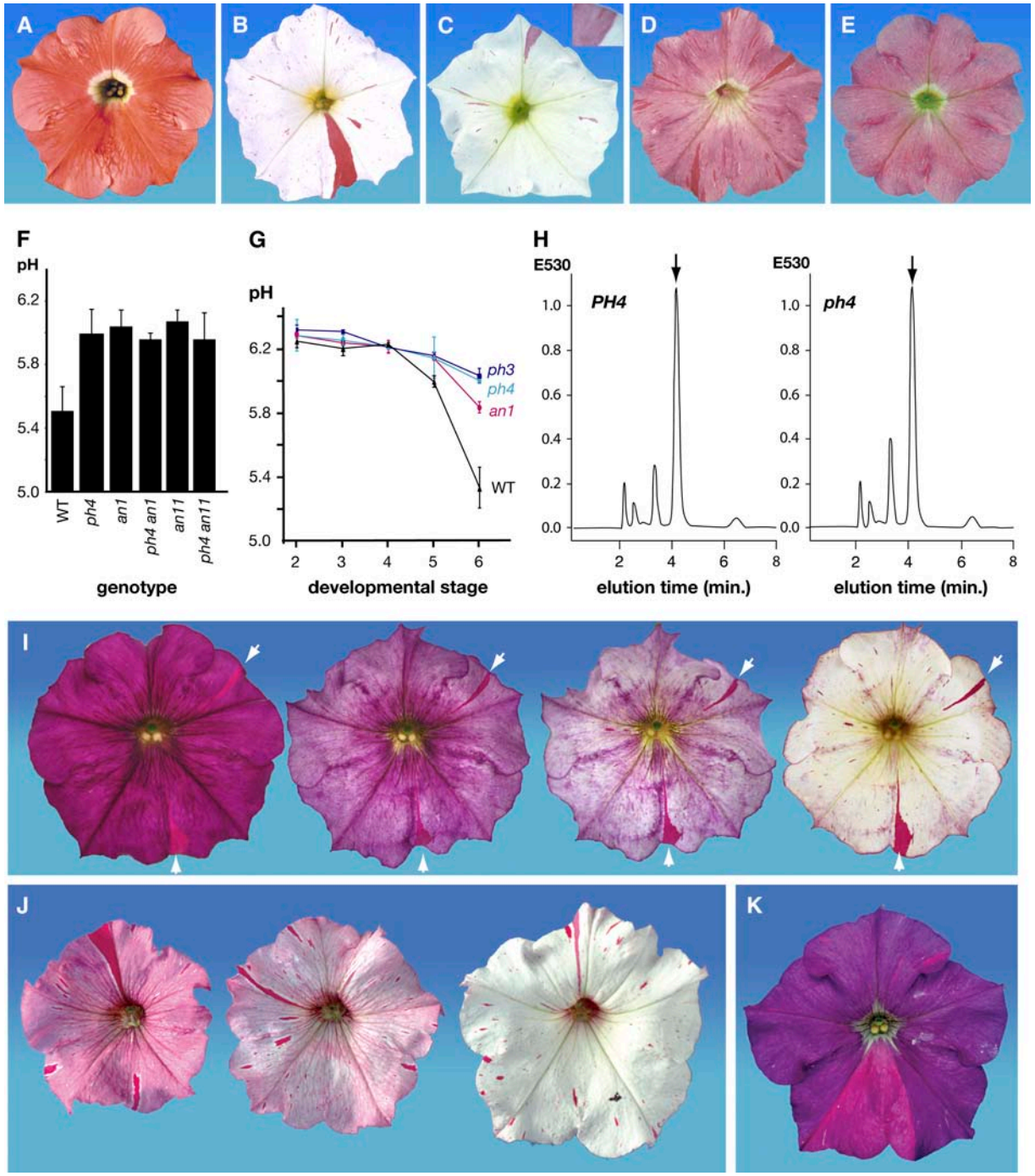

Figure 2. Phenotypic Analysis of Flower Pigmentation Mutants.

(A) Flower of the wild-type line R27 (*AN1, AN11, PH4*).

(B) Flower of the line W137 (*an11-W137, PH4*) showing *AN11-R* revertant sectors, resulting from excisions of *dTPH1*, on a white (*an11-W137*) background.

(C) Flower homozygous for the unstable alleles *an11-W137* and *ph4-B3021*. Reversion of *an11-W137* results in spots with a purplish color rather than red, as a result of the *ph4-B3021* mutation. Somatic reversions of *ph4-B3021* can be seen occasionally as red (*PH4-R*) spots within the purplish *ph4-B3021* sectors (inset).

(D) Flower of line R154 harboring the unstable *ph4-V2166* allele in an *AN1-R AN11-R* background. Note the red *PH4* revertant sectors on the purplish *ph4* background.

(E) Flower of line R149 harboring the stable recessive *ph4-V2153* allele in an *AN1-R AN11-R* genetic background.

(Figure 3C) and *ph4-V2166* (Figure 3D) showed that reversion of the *ph4* phenotype correlated with excision of *dTPH1* from *MYBa*.

DNA analyses of plants containing *ph4-X2052* or *ph4-C3540*, either in homozygous or heterozygous condition, showed that these mutants also contained *dTPH1* insertions in *MYBa*, whereas the stable recessive *ph4-V2153* mutants contained an ~4-kb *TPH6* insertion that is nearly identical to the *TPH6* element found in the alleles *an1-W17* and *an1-W219* (Spelt et al., 2002) (Figure 3B). Plants harboring the weakly unstable *ph4-X2377* allele contained a 177-bp insertion 29 bp downstream from the translation start site. The insertion is flanked by an 8-bp target site duplication and has a 12-bp terminal inverted repeat with similarity to the terminal inverted repeats of *hAT* family transposons, including *dTPH1* and *Activator* from maize. Because the internal sequences of the insertion show no similarity to other transposons and are too short to encode a transposase, it apparently represents a new (sub)family of nonautonomous petunia transposons that we named *dTPH7*. The *ph4* lines V64 and M60 both contain a *dTPH1* insertion in *MYBa* in exactly the same position (Figure 3B).

In summary, these data show that mutations in the isolated gene (*MYBa*) fully correlate with the phenotype conferred by the *ph4* mutant, implying that *PH4* is identical to *MYBa*. Below, we refer to this gene as *PH4*.

PH4 Encodes a MYB Domain Protein

Sequence analysis of a full-size *PH4* cDNA and the corresponding genomic region showed that the *PH4* mRNA is encoded by two exons separated by a 715-bp intron (Figure 3B). The cDNA contains a single large open reading frame encoding a 291–amino acid protein. Database searches showed that a 103–amino acid domain, located near the N terminus, is conserved in a large number of plant and animal proteins all belonging to the MYB family of transcription factors (Figures 4A and 4B). The MYB domain consists of one, two, or three helix-helix-turn-helix motifs that potentially bind DNA. PH4, like the majority of plant MYBs (Stracke et al., 2001), contains only the repeats R2 and R3 (Figure 4B).

R2R3 MYB genes constitute a large family of ~125 genes in *Arabidopsis* and >85 genes in rice (*Oryza sativa*) and have been categorized into 42 subgroups based on similarities in the encoded proteins and intron–exon structures (Stracke et al., 2001; Jiang et al., 2004). Generally, sequence similarity between MYB proteins is restricted to the N-terminal MYB domain, but 19 subgroups of R2R3 MYBs share some conserved motifs in their C-terminal domains that may indicate similarities in function (Stracke et al., 2001; Jiang et al., 2004).

PH4 is most similar to the R2R3 MYB proteins BNLGHi233 from upland cotton (*Gossypium hirsutum*), MYBCS1 and MYB5 from grape (*Vitis vinifera*), MYB5 from *Arabidopsis*, and MYB4 from rice (Figure 4A). The clustering of R2R3 MYBs in Figure 4 is in good agreement with previous analyses based on a much larger set of MYBs (Stracke et al., 2001; Jiang et al., 2004) and extends the data at some points. For example, grape MYBA1 and tomato (*Solanum lycopersicum*) ANT1, recently identified regulators of the anthocyanin pathway in grape (Kobayashi et al., 2004) and tomato (Mathews et al., 2003), respectively, cluster with known members (AN2 of petunia, PAP1 and PAP2 of *Arabidopsis*) of subgroups 6 and N9 as defined by Stracke et al. (2001) and Jiang et al. (2004), respectively. Curiously, C1 and Pl, regulators of the anthocyanin pathway in maize, cluster in a distinct group (5/N8) together with TT2, a regulator of proanthocyanidin and anthocyanin synthesis in *Arabidopsis* (Shirley et al., 1995), again consistent with previous results.

ODO1, an activator of the synthesis of phenylpropanoid volatiles in petunia flowers, clusters with *Arabidopsis* MYB42 and MYB85, similar to previous results (Verdonk et al., 2005), but it does not contain the conserved motif found in the C termini of MYB42 and MYB85 (Jiang et al., 2004).

Figure 4B shows that PH4, *Arabidopsis* MYB5, *grape* MYBCS1 and MYB5, cotton BNLGHi233, and rice MYB4 share two conserved motifs in their C-terminal domains. Such motifs have been used as signatures for the classification of subgroups (Stracke et al., 2001; Jiang et al., 2004). Given that these C-terminal motifs in PH4 and related R2R3 MYBs are much better conserved than those in proteins of subgroup N9, we propose that these MYBs form a new subgroup that we tentatively named G20, in accordance with the numbering of Jiang et al. (2004). This classification

Figure 2. (continued).

(F) pH values (means ± SD; $n = 7$) of petal homogenates of different genotypes in the R27 genetic background. Note that the absolute pH values that are measured show some variation in time, possibly in response to variable environmental conditions in the greenhouse, although the differences between mutants and the wild type are virtually constant.

(G) Petal homogenate pH (means ± SD; $n = 5$) during flower development in wild-type, *an1*, *ph3*, and *ph4* petals. Developmental stages were defined as follows: stage 2, 30- to 35-mm buds; stage 3, 35- to 45-mm buds; stage 4, buds of maximum size (45 to 50 mm); stage 5, unfolding flowers; stage 6, fully open flowers around anthesis.

(H) HPLC analysis of methanol-extractable anthocyanins in petals of stage 4 flower buds from lines R27 (*PH4*) and R149 (*ph4-V2153*). The arrows denote the retention time of cyanidin 3-glucoside.

(I) Phenotype of *ph4-V2166/ph4-V64* flowers in a background that allows the synthesis of 3RGac5G-substituted anthocyanins, resulting from the cross R149 × V64, showing subsequent stages (from left to right) of flower color fading. Note that the blue-violet *ph4* cells fade, whereas the red-violet *PH4* revertant sectors (white arrows) do not.

(J) Phenotype of *an1-G621/an1-W138* flowers in a background that synthesizes 3RGac5G-substituted anthocyanins, showing subsequent stages (from left to right) of flower color fading. Note that mutant (*an1-G621*) tissues fade, whereas full *AN1* revertant sectors (mostly originating from excisions of *dTPH1* from *an1-W138*) do not fade.

(K) Phenotype of a mature *ph2-A2414* flower (comparable to the rightmost flowers in **[I]** and **[J]**) in a background (R160 × V26) that synthesizes 3RGac5G-substituted anthocyanins. Note that neither the *PH2* tissue (red-violet sectors) nor the *ph2* tissue (blue-violet background) displays fading.

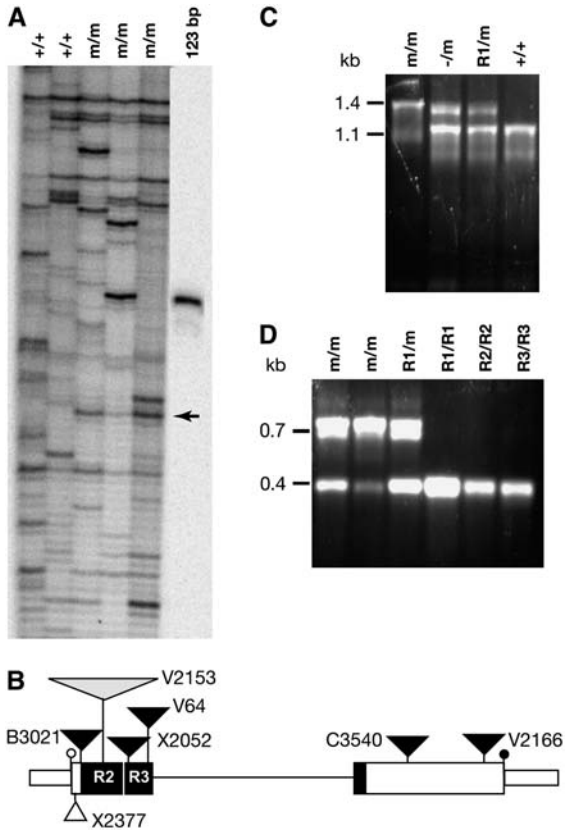

Figure 3. Molecular Analysis of *PH4*.

(A) Transposon display analysis of plants homozygous for the parental wild type (+/+) or the mutable *ph4-B3021* allele (m/m). The rightmost lane contains a radiolabeled 123-bp size marker. The arrow indicates a fragment derived from *PH4*.

(B) Map of the *PH4* gene and mutant alleles. Boxes represent exons, and the thin line represents an intron. Protein-coding regions are indicated by double height, and the region encoding the R2 and R3 repeats of the MYB domain is filled in black. The open and closed circles represent the start and stop codons, respectively. The triangles indicate transposon insertions in the indicated alleles: the large open triangle represents *TPH6*, the mid-size closed triangles represent *dTPH1*, and the small open triangle represents *dTPH7*.

(C) PCR analysis of plants harboring *ph4-B3021* and derived stable *ph4* alleles. + indicates the parental wild-type allele, m indicates the mutable *ph4-B3021* allele, R1 indicates a derived revertant allele, and – indicates a stable recessive *ph4* allele. The primers used were 583 and 1060 (Table 1).

(D) PCR analysis of plants harboring *ph4-V2166* and derived germinal revertant alleles. m represents the mutable *ph4-V2166* allele, and R1, R2, and R3 represent three independently isolated revertant alleles. The primers used were 690 and 582.

is supported by the finding that both *Arabidopsis* MYB5 and PH4 contain only one intron (Li et al., 1996) (Figure 3), whereas the majority of R2R3 MYBs contain two (Jiang et al., 2004).

Yeast two-hybrid assays showed that *Arabidopsis* MYB5 (Zimmermann et al., 2004) and PH4 (see below) can interact physically with functionally similar BHLH proteins, consistent with the idea that they have similar functions. However, the expression pattern of MYB5 (Li et al., 1996) seems quite different from that of PH4 (see below). Rice MYB4 induces freezing and chilling tolerance when constitutively expressed in *Arabidopsis* (Vannini et al., 2004), and grape MYB5 induces the synthesis of anthocyanins and proanthocyanidins when overexpressed in tobacco (*Nicotiana tabacum*) (Deluc et al., 2006). Definite proof for functional equivalence and/or orthology will require the swapping of genes between species and/or the identification of (direct) target genes (see Discussion).

Expression of *PH4* and Mutant Alleles

To determine the expression pattern of *PH4*, we measured the amount of *PH4* mRNAs in different tissues of the wild-type line V30 by RT-PCR. We used line V30 because it contains functional alleles of all regulatory pigmentation genes (Koes et al., 1986), whereas R27 is mutant for *an4*, a regulator of anthocyanin synthesis and *AN1* expression in anthers (Quattrocchio et al., 1993; Spelt et al., 2000). Figure 5A shows that *PH4* is relatively strongly expressed in the limb of the petal, whereas in the tube only weak *PH4* expression is detected. Possibly, the low amount of transcripts in the tube sample originated from cells near the border of the limb and the tube. The expression in the limb reaches a maximum at developmental stages 5 to 6 (Figure 5A), when the bud is opening, which correlates with the moment that pH differences were first seen between wild-type and *ph4* petal limb extracts (Figure 2E).

Ovaries are the only other tissue besides petals in which we detected clear *PH4* expression. This organ also expresses *AN1* (Figure 5A) (Spelt et al., 2000), which directs the activation of the anthocyanin biosynthetic gene *DFR*, but for unknown reasons this does not result in the accumulation of anthocyanin pigments (Huits et al., 1994).

Anthers of V30 are pigmented by anthocyanins and express *AN1* mRNA during early stages of development (stages 1 to 3). However, no *PH4* transcripts were detected in this tissue. The same holds for the stigma and style. *AN1* is weakly expressed in sepals, leaves, and stems of V30, which correlates with the synthesis of low amounts of anthocyanin; *PH4*, however, is not expressed in these tissues. Roots are normally not pigmented and do not express *PH4* or *AN1*.

To examine to what extent the transposon insertions affected the expression of *PH4*, we analyzed *ph4* mRNAs in petal limbs of different mutants by RNA gel blot analysis, RT-PCR (data not shown), and rapid amplification of 3′ cDNA ends (3′RACE). Figure 5B shows that the amount of *PH4* transcripts in petal limbs homozygous for the *ph4* alleles *X2052*, *B3021*, *C3540*, and *V2166* is strongly reduced compared with that of the isogenic wild-type line R27. The same holds for *PH4* transcripts expressed from the *X2377* allele compared with an isogenic revertant (*ph4-X2377R*). Presumably, the *dTPH1* insertions in these alleles result in highly unstable mRNAs that are rapidly degraded. The small amount of wild-type-size *PH4* transcripts in these corollas presumably originates from cells in which *dTPH1* was excised from *PH4*.

The insertions in *ph4-V64* and *ph4-V2153* cause the accumulation of short *ph4* transcripts. Cloning and sequencing of these products revealed that they resulted from polyadenylation within the *dTPH1* and *TPH6* sequences, respectively, and encode

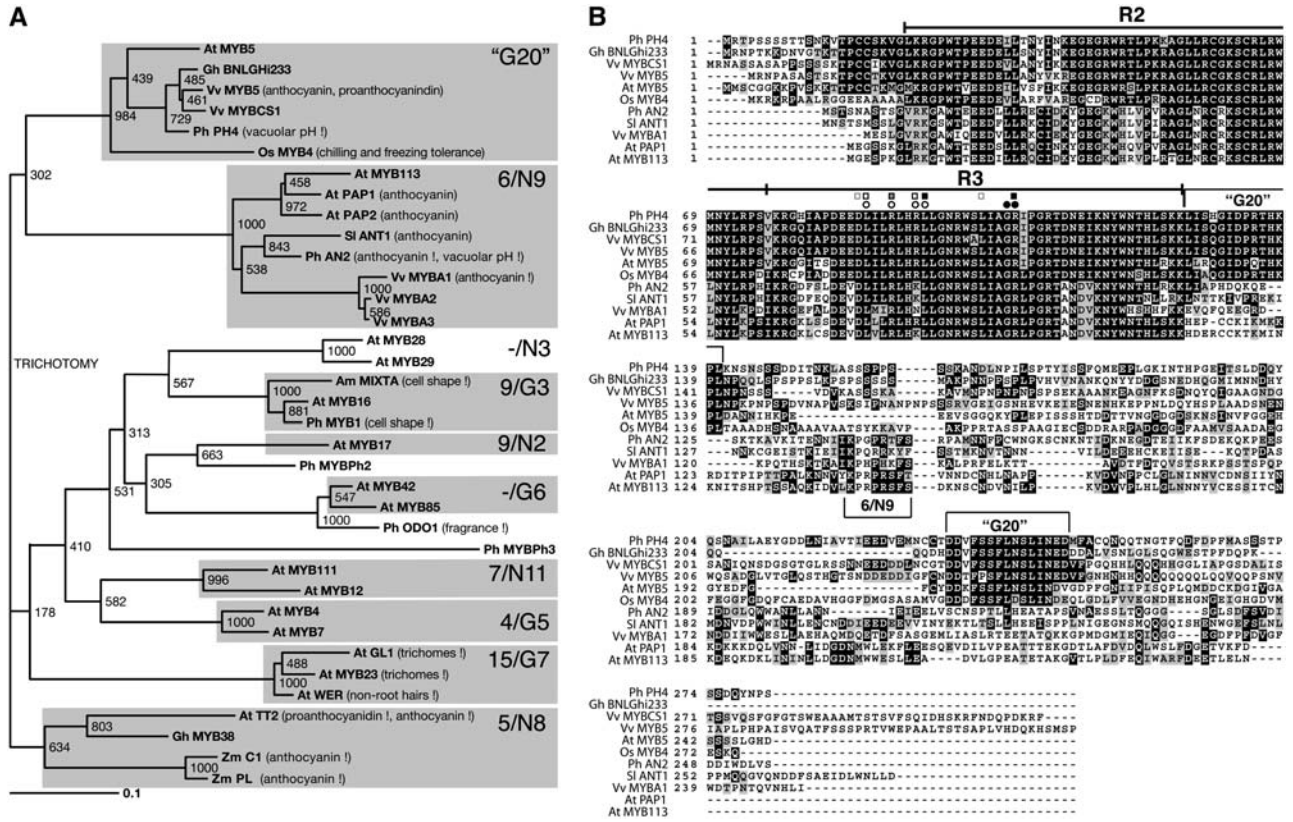

Figure 4. Similarity of PH4 to Other MYB Proteins.

(A) Phylogenetic tree displaying the similarity of PH4 to other R2R3 MYB proteins. The tree was based on an alignment of the 104 amino acids spanning the MYB domain (see Supplemental Figure 2 online). Names of the various proteins are given in boldface uppercase letters, and their origin is indicated by a two-letter prefix: Am is *Antirrhinum*, Ph is petunia, At is *Arabidopsis*, Zm is maize, Sl is tomato, Vv is grape, and Gh is cotton. The function of some of the proteins is given in parentheses and, if substantiated by a loss-of-function phenotype, an exclamation point. The gray boxes indicate representatives of subgroups of related R2R3 MYB proteins defined previously (Stracke et al., 2001; Jiang et al., 2004); proteins in subgroups with G numbers share conserved sequences in their C termini, whereas proteins in subgroups with N numbers do not (Jiang et al., 2004). Because R2R3 MYBs from the PH4 subgroup share sequence similarity in their C termini, they are classified as a new G subgroup that we tentatively labeled ''G20.'' Numbers at branch points indicate bootstrap support (1000 replicates).

(B) Alignment of PH4 to R2R3 MYB proteins of subgroups N9 and G20. Identical amino acids are indicated in black, similar amino acids in gray. Dashes represent gaps introduced to improve the alignment. The R2 and R3 repeats that make up the MYB domain are indicated above the alignment. Regions in the C-terminal domains that are conserved between members of the N9 and G20 subgroups are boxed. Amino acids homologous with residues in maize C1 that are required for physical interaction with R and for R-dependent transcriptional activation (Grotewold et al., 2000) are indicated above the sequence with white and black circles, respectively. Amino acids in *Arabidopsis* TT2 that are involved in the interaction with a BHLH partner and/or the activation of the *DFR* promoter (Zimmermann et al., 2004) are indicated with squares: residues with strong effect on TT2 activity when mutated are indicated by black squares, and those with mild or small effect are indicated by gray and white squares.

truncated PH4 proteins that contain only part of the DNA binding and protein–protein interaction domains. Although truncations of transcription factors can have dominant-negative effects (Singh et al., 1998; Ferrario et al., 2004), this is apparently not the case here, as *ph4-V64* and *ph4-V2153* are recessive mutations.

PH4 Interacts with AN1 and JAF13

To analyze the mechanism by which AN1 regulates anthocyanin synthesis and intracellular pH, we used the yeast two-hybrid system to search for proteins that interact with AN1. Therefore, we constructed a plasmid that expresses a bait protein consisting of the conserved 238 N-terminal amino acids of AN1 fused to the DNA binding domain of GAL4 ($AN1^{1-238}GAL4^{BD}$) and screened a yeast two-hybrid cDNA library made from R27 petal RNA.

In 23 of 5×10^5 yeast transformants, the introduction of the cDNA plasmid resulted in reproducible activation of the GAL4-responsive *HIS3* and *ADE2* reporter genes, resulting in His and adenine auxotrophy. Sequence analysis showed that these 23 transformants contained cDNAs derived from four different genes, all encoding MYB proteins. Seventeen clones contained partial cDNAs from *PH4*, and three clones contained partial cDNAs of *AN2*. The three remaining clones encode two MYB

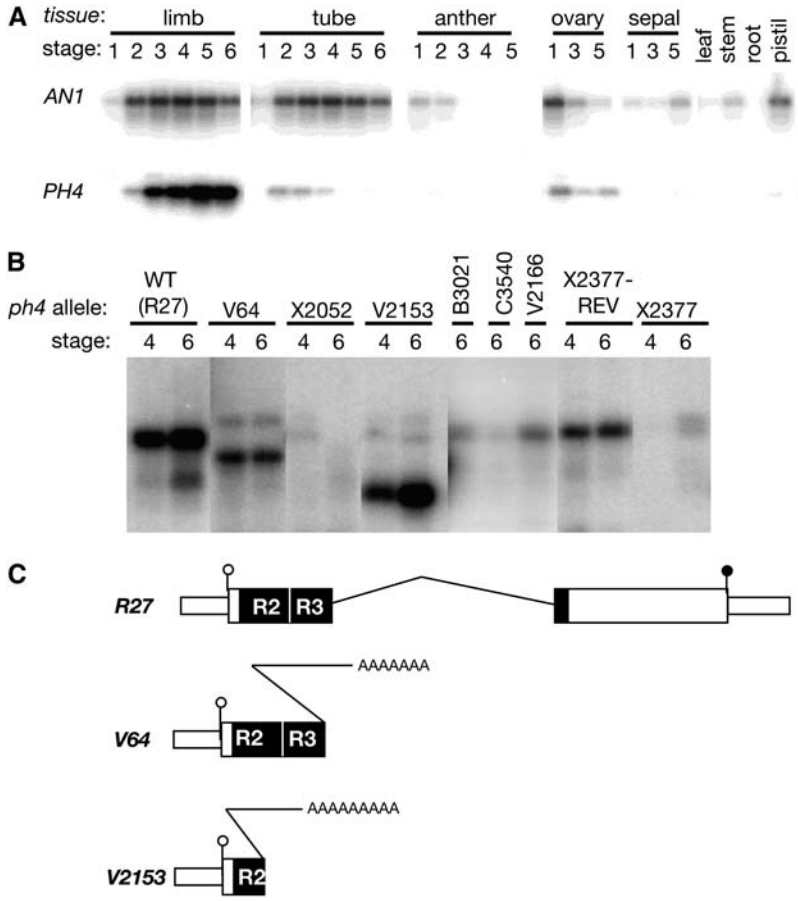

Figure 5. Expression Analysis of *PH4*.

(A) RT-PCR analysis of *PH4* and *AN1* mRNAs from organs (petal limbs, petal tubes, anthers, ovaries, and sepals) of flowers of different developmental stages (1 to 6) and from leaves, roots, stems, and stigma plus style.

(B) 3′RACE analysis of mRNAs expressed from mutant *ph4* alleles. RNA was isolated from petals of stages 4 and 6 flowers homozygous for different *ph4* alleles, as indicated above the lanes. RT products were amplified with a primer complementary to the 5′ untranslated mRNA region immediately upstream of the start codon (primer 1107) and the poly(A) tail.

(C) Structure of mutant *ph4* mRNAs. The exons and protein-coding regions are drawn as in Figure 3B. The half-triangles with poly(A) at the 3′ ends of *ph4-V64* and *ph4-V2153* mRNAs denote *dTPH6* and *dTPH1* sequences, respectively.

domain proteins (named MYBb1 and MYBx) that had not been identified previously (Kroon, 2004). A detailed functional analysis of the latter will be published elsewhere.

To analyze the two-hybrid interaction between PH4 and AN1 in more detail, we made new constructs to express the full PH4 ($PH4^{1-291}$) and AN2 ($AN2^{1-255}$) proteins as fusions to either the activation domain of GAL4 ($GAL4^{AD}$) or $GAL4^{BD}$ (Figure 6A). When expressed (alone) in yeast, $PH4^{1-191}GAL4^{BD}$ and $AN2^{1-255}GAL4^{BD}$ strongly activated the GAL4-activated *HIS3*, *ADE*, and *LACz* reporter genes, whereas $GAL4^{BD}$ did not, suggesting that PH4 and AN2 both contain a strong transcription activation domain, as was shown previously for C1 from maize (Goff et al., 1991). Because of the autoactivation of PH4-$GAL4^{BD}$ and AN2-$GAL4^{BD}$ fusions, we used instead fusions to $GAL4^{AD}$ to analyze two-hybrid interactions with AN1 and JAF13.

Figure 6B shows that a fusion of full PH4 to $GAL4^{AD}$ ($PH4^{1-291}GAL4^{AD}$) interacts in a two-hybrid assay with $GAL4^{BD}$ fusions containing full AN1 or its conserved N-terminal domain ($AN1^{1-668}GAL4^{BD}$ and $AN1^{1-238}GAL4^{BD}$), but not with $GAL4^{BD}$ alone. Subsequent biochemical experiments showed that in vitro translated AN1 and PH4 could be coimmunoprecipitated with an anti-AN1 serum, confirming that the observed two-hybrid response resulted from a direct physical interaction between both proteins (see Supplemental Figure 3 online). The interaction between PH4 and AN1 appeared equally strong as that between AN2 and AN1, because both combinations activated the *ADE2* and *LACz* genes to a similar extent. Furthermore, AN2 and PH4 interacted with similar efficiency with the N-terminal domain of JAF13, as they did with the same domain of AN1.

When tested separately, we found that the C termini of AN2 and PH4 ($PH4^{127-291}$ and $AN2^{115-255}$) did not interact at all with AN1 or JAF13, whereas the N-terminal parts containing the MYB domain (PH^{1-134} and $AN2^{1-121}$) gave a weak two-hybrid response that could be unambiguously scored with the ADE reporter but

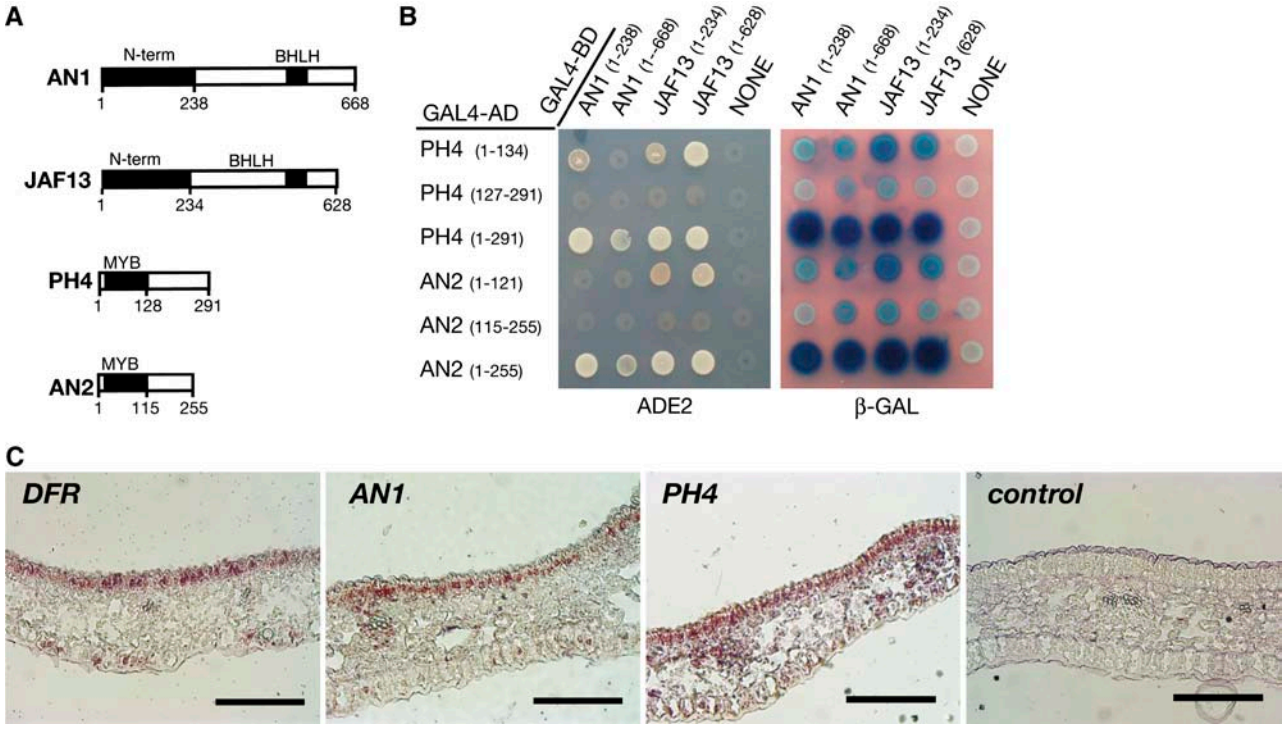

Figure 6. Interactions between PH4 and Regulators of the Anthocyanin Pathway.

(A) Diagrams of the proteins showing the positions of conserved domains (black) used for the two-hybrid analysis. The numbers below each map indicate the positions of amino acid residues.

(B) Yeast two-hybrid analysis. Different combinations of plasmids expressing fusion proteins (as indicated at left and at bottom of the grids) were cotransformed in yeast, spotted on a plate, and assayed for simultaneous activation of the *HIS* and *ADE* reporter genes (seen as His- and adenine-independent growth; left panel) or the *LACz* reporter gene (seen as bluing in an X-Gal overlay assay; right panel).

(C) In situ localization of *AN1*, *PH4*, and *DFR* mRNAs in the petal limb, detected by hybridization with antisense RNA probes. As a negative control, sections were hybridized with a sense strand of *DFR* (control). Sections are depicted with the adaxial epidermis at the top. Bars = 100 μm.

was barely detectable with the *LACz* reporter (Figure 6B). The weak response of the separated AN2 and PH4 domains relative to the full proteins may result from (1) a reduced transcription activation potential of $PH4^{1-134}$ and $AN2^{1-121}$complexes relative to the full proteins, attributable to the removal of the strong transcription activation domain in their C termini, (2) aberrant folding of the isolated MYB domains, and/or (3) the MYB regions containing only part of the interaction domain.

A detailed characterization of maize C1 (Grotewold et al., 2000) and *Arabidopsis* PAP1 (Zimmermann et al., 2004) identified several amino acids in the first helix of the R3 domain that are critical for the interaction with their BHLH partner (R and EGL3, respectively) and/or the transcription activation of downstream genes. These residues are conserved in AN2 and PH4 (Figure 4B) and may play a critical role in the interaction with AN1 and JAF13 and the activation of downstream genes.

To assess whether PH4 and AN1 might be able to form complexes in vivo, we performed in situ hybridization analysis to examine whether *PH4* and *AN1* are coexpressed in the same petal cells. Figure 6C shows that *DFR* is expressed in the upper (adaxial) epidermis of the corolla and at a much lower level in the lower (abaxial) epidermis, consistent with the anthocyanin pigmentation pattern. *AN1* mRNA was expressed in a very similar pattern: relatively high expression is seen in the upper epidermis, and lower expression (just above the detection limit) is seen in the lower epidermis. *PH4* mRNA could be detected clearly in the upper epidermis. However, because of the low expression levels of *PH4* mRNA, it was difficult to differentiate the weak colorigenic signals that were sometimes observed in the lower epidermis or the mesophyll from the background signal that results from nonspecific binding of the probe. Hence, we cannot exclude or confirm that *PH4* is also weakly expressed in these cells. Together, these findings indicate that AN1 and PH4 may form complexes in the upper epidermis of the flower corolla, which are the same cells in which the color change is seen in *an1* and *ph4* mutants.

PH4 and AN1 Regulate Overlapping Sets of Target Genes

Given that AN2 and PH4 are both MYB proteins that can interact with AN1 and JAF13, we addressed the question of how (dis)-similar they are functionally. AN2 coregulates with AN1 and AN11 the expression of at least eight structural anthocyanin genes in the petal limb (Quattrocchio et al., 1993) and may also play a role in the transcription of AN1 (Spelt et al., 2000).

To test directly whether *PH4* is involved in the expression of structural anthocyanin genes, we measured the amount of several

of their mRNAs in wild-type (R27) and isogenic *an1-W225* and *ph4-V2153* petals. Figure 7A shows that in *an1* petal limbs the structural genes *CHS*, *CHI*, and *F3H* are normally expressed, whereas the expression of *DFR*, *AS* (encoding anthocyanin synthase [Weiss et al., 1993]), *AAT* (encoding an anthocyanin-rutinoside acyltransferase; Brugliera and Koes, 2001; F. Brugliera and R. Koes, unpublished data), and *AN9* (encoding a glutathione transferase–like protein; Alfenito et al., 1998) is strongly reduced. However, the *ph4* mutation has no clear effect on any of these mRNAs. This finding indicates that *PH4* plays no role in the regulation of anthocyanin genes, or that its role is redundant with that of another gene.

To discriminate between these possibilities, we analyzed the activity of PH4 in a gain-of-function assay. We introduced a *PH4* gene construct driven by the constitutive 35S promoter of *Cauliflower mosaic virus* (*35S*:*PH4*) into leaf cells by particle bombardment and measured its capacity to activate a *LUCIFERASE* (*LUC*) reporter driven by the promoter of *DFR* (*DFR*:*LUC*). In these experiments, we cobombarded a β-*GLUCURONIDASE* (*GUS*) reporter gene driven by the 35S promoter (*35S*:*GUS*) to correct for variations in transformation efficiency. Figure 7B shows that the *DFR:LUC* reporter showed little or no expression in leaf cells when introduced alone. Consistent with earlier results (Spelt et al., 2000, 2002), the expression of *DFR:LUC* was strongly induced (>35-fold) when it was cointroduced with *35S*:*AN1* and *35S*:*AN2*. However, when *35S*:*AN2* was replaced by *35S*:*PH4*, the *DFR*:*LUC* reporter was not induced, nor was it when we cointroduced *35S*:*JAF13* in addition. These findings show that for activation of the *DFR* promoter, AN2 cannot be replaced by PH4, suggesting that PH4 plays no role in the transcriptional activation of *DFR*.

To unravel the nature of the acidification pathway that is activated by PH4, we analyzed transcripts expressed in wild-type, *an1*, *ph3*, *ph4*, and *ph5* petals by microarray and cDNA-AFLP analysis and identified nine mRNA fragments whose expression is reduced in *an1* and *ph4* petals (a full account of these experiments will be published elsewhere). One of the identified mRNAs, named *CAC16.5* (for *cDNA-AFLP clone 16.5*), encodes a Cys proteinase–like protein (GenBank accession number AY371317) (see Supplemental Figure 4 online). Figure 7A shows that *CAC16.5* mRNA is strongly reduced in *an1* and *ph4* petals compared with wild-type petals, indicating that *CAC16.5* expression requires both AN1 and PH4.

To examine the role of AN2 in *CAC16.5* expression, we analyzed *CAC16.5* mRNAs in *an2* petals and isogenic controls in which the *an2* mutation was complemented by a *35S*:*AN2* transgene. Figure 7C shows that the restoration of flower pigmentation by *35S*:*AN2* was accompanied by strong (re)induction of *DFR* mRNA expression, consistent with previous results (Quattrocchio et al., 1998; Spelt et al., 2000). However, the expression of *CAC16.5* and *PH4* mRNA was similar in *an2* and

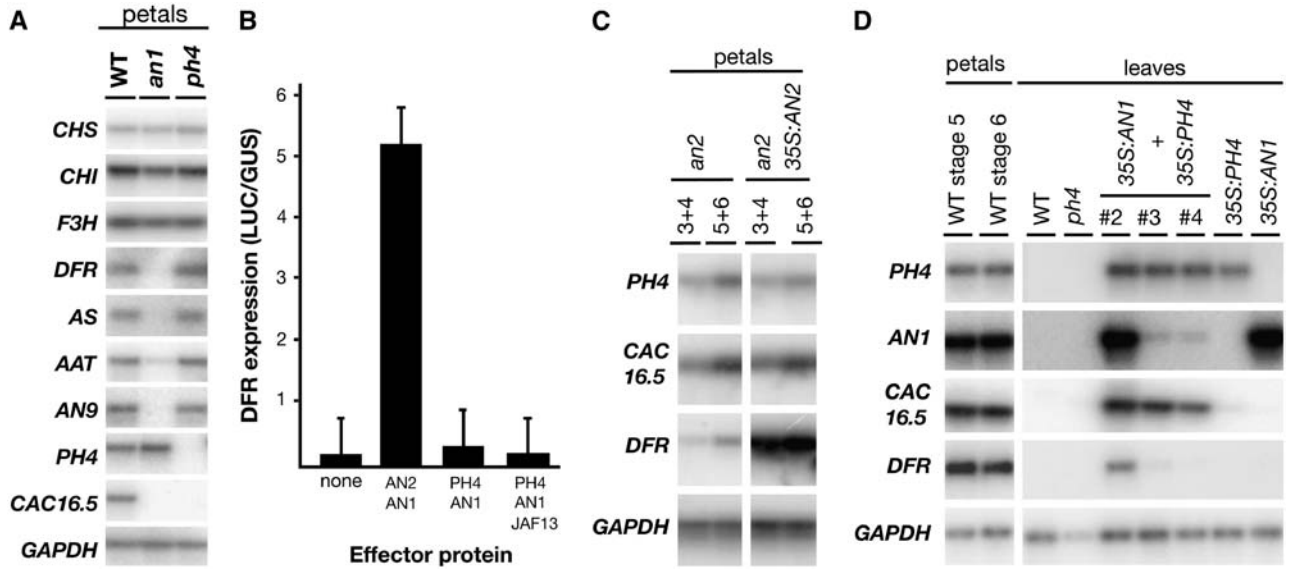

Figure 7. Effect of *PH4* Function on Gene Expression.

(A) RT-PCR analysis of various mRNAs (indicated at left) expressed in petals of the wild type (R27) and stable *an1-W225* and *ph4-V2153* mutants.
(B) Activation of a *DFR*:*GUS* reporter gene in transiently transformed leaf cells. The columns and error bars denote means ± SD ($n = 8$) of *DFR:LUC* expression after cobombardment with various combinations of *35S*:*AN1*, *35S*:*AN2*, *35S*:*JAF13*, and/or *35S*:*PH4. DFR:LUC* expression (in arbitrary units) was measured as LUC activity and normalized to GUS activity expressed from a cobombarded reference gene (*35S*:*GUS*).
(C) RT-PCR analysis of mRNAs (indicated at left) expressed in petals of *an2* mutants and isogenic transgenic plants in which *an2* is complemented by a *35S*:*AN2* transgene. Petals of closed buds (stage 3+4) and open(ing) flowers (stage 5+6) were analyzed.
(D) Gene expression in wild-type, *an1*, and *ph4* petals and leaves of transgenic plants containing *35S*:*AN1* and/or *35S*:*PH4*. The expression levels of the mRNAs (indicated at left) were determined by RT-PCR. The genotype of each sample is indicated above the lane. Three distinct double transgenic plants (containing *35S*:*AN1* and *35S*:*PH4*) were analyzed that differ in the strength of *35S*:*AN1* expression (designated #2, #3, and #4).

an2 35S:AN2 petals, indicating that AN2 has little or no effect on *CAC16.5* or *PH4* expression.

To examine the regulation of *CAC16.5* by PH4 and AN1 in further detail, we analyzed transgenic plants containing *35S:PH4* and *35S:AN1*. Figure 7D shows that *CAC16.5* and *DFR* mRNAs are not expressed in wild-type leaves. Although the *35S:PH4* line expresses similar amounts of *PH4* mRNA in leaves as the endogenous *PH4* gene does in petals, this results only in a very weak activation of *CAC16.5* in leaves, to a level that is barely visible in Figure 7D. Although the *35S:AN1* line expressed *AN1* mRNA in leaves to a level that is twofold to threefold higher than that found in wild-type petals, no induction of *CAC16.5* or *DFR* mRNA was observed. Thus, both AN1 and PH4 are on their own insufficient to induce *DFR* or *CAC16.5* efficiently.

To obtain plants that ectopically express AN1 and PH4, we crossed the *35S:AN1* and *35S:PH4* lines. The *35S:PH4* parent used apparently contains multiple active copies of the transgene, because after crossing to other empty lines, all 84 progeny contained and expressed a *35S:PH4* transgene. The *35S:AN1* parent (Spelt et al., 2000), however, contained a single active transgene locus that segregated as a single Mendelian factor in crosses. After crossing the *35S:PH4* and *35S:AN1* parents, all 39 progeny contained *35S:PH4*, whereas only 4 of them contained *35S:AN1* (plants 1 to 4). Plant 1 grew very poorly and died before it could be subjected to more detailed analyses. Plant 2 grew slowly, remained severely stunted, and bore leaves with a weak and patchy anthocyanin pigmentation pattern (see Supplemental Figure 5 online). Plants 3 and 4 developed normally. Moreover, leaf extracts of plant 2 were significantly more acidic than those of plants 3 and 4 or control plants that had not been transformed. RT-PCR analysis showed that plant 2 expressed the *35S:PH4* and *35S:AN1* gene in leaves to a similar extent as the parental lines did. In plants 2 and 3, however, the expression of *35S:AN1* was significantly reduced compared with the parental *35S:AN1* line, possibly as a result of (epigenetic) silencing of the transgene. Together, it appears that strong, ectopic coexpression of AN1 and PH4 has a deleterious effect, possibly attributable to ectopic activation of a vacuolar acidification pathway.

Despite the low expression of *35S:AN1* in plants 3 and 4, *CAC16.5* RNA was induced in their leaves to levels that are close to *CAC16.5* mRNA in petals, whereas *DFR* was hardly induced at all. In plant 2, however, the induction of *CAC16.5* was even stronger than in leaves of plants 3 and 4; moreover, *DFR* was clearly activated, although the actual mRNA levels remained far lower than in petals. Given the aberrant phenotype of plant 2, we cannot distinguish whether the activation of *DFR* is a direct effect of AN1 and PH4 expression or an indirect (stress) effect caused, for example, by the physiological changes that are induced by AN1 and PH4 (see Discussion).

DISCUSSION

The BHLH and WD40 regulators AN1 and AN11 activate, in addition to anthocyanin synthesis, several other aspects of epidermal cell differentiation, such as growth and division of cells in the seed coat epidermis and vacuolar acidification in petals (Spelt et al., 2002). Here, we present evidence that AN1 activates these processes through interactions with two distinct MYB proteins encoded by *AN2* and *PH4*.

Control of Vacuolar Acidification and Flower Color Fading

Previous analyses of *PH4* and *ph4* mutants in heterogeneous genetic backgrounds indicated that the *ph4* mutation causes a more bluish flower color and increases the pH of petal limb homogenates (de Vlaming et al., 1983). Analyses of *PH4* and *ph4* flowers in an isogenic background confirm and extend these findings.

In the R27 genetic background (*rt*/*rt*), the *ph4* mutation does not affect the expression of structural anthocyanin genes or the accumulation of anthocyanin pigments, suggesting that the color change is attributable largely to the effect on vacuolar pH (Figure 2). However, in a genetic background containing *RT* (to allow the synthesis of 3RGac5G-substituted anthocyanins) and the dominant *FADING* allele (de Vlaming et al., 1982), *ph4* or *an1-G621* triggers the almost complete disappearance of anthocyanins in the petals and the fading of the flower color after opening of the bud (Figure 2).

The dependence of fading on a dominant *FA* allele and a 3RGac5G substitution pattern of the anthocyanins suggests that fading may involve an active (enzymatic) substrate-specific degradation process. However, because *FA* is not isolated and because the origin of the *FA* and *fa* alleles is unclear, it cannot be ruled out that *FA* is actually a dominant-negative allele and that the recessive *fa* allele encodes an active protein required for the stability of anthocyanins. Furthermore, it cannot be excluded that fading does not depend on the genes *RT* and *GLYCOSYLATION AT FIVE* (*GF*) and the resulting 3RGac5G anthocyanin substitution pattern but on distinct genes that are genetically linked to *RT* and *GF*. Consequently, the molecular role of *PH4* in (preventing) fading is difficult to infer at this stage. Because *ph2* and *ph5* mutations increase vacuolar pH without inducing fading, it is possible that fading in *ph4* and *an1* is not attributable to a less acidic vacuolar lumen alone but depends on an additional defect in vacuolar physiology.

Given that PH4 is a MYB domain protein that can interact with the transcription factors AN1 and JAF13, it presumably activates vacuolar acidification indirectly, by regulating the transcription of downstream genes that encode proteins involved in proton metabolism. We consider it unlikely that PH4 activates the expression of one or more subunits of a v-ATPase proton pump, because mutations that inactivate v-ATPase were shown to cause severe developmental defects and often lethality in a variety of species (Davies et al., 1996; Ferea and Bowman, 1996; Inoue et al., 1999; Schumacher et al., 1999; Oka and Futai, 2000; Strompen et al., 2005). Moreover, immunoblot analysis showed that the v-ATPase A and B subunits as well as pyrophosphatase proteins are expressed at equal levels in *PH4* and *ph4* petals (N. Frange and E. Martinoia, unpublished data).

To determine the nature of the vacuolar pathway downstream of AN1 and PH4, we started the analysis of transcripts that are expressed at reduced levels in *an1* and/or *ph4* mutants. One of these is *CAC16.5*, which encodes a protein homologous with Cys proteinases that is expressed in petals but not in leaves. The *CAC16.5* expression domain is largely determined by AN1 and

PH4, as the gene is inactivated in *an1* and *ph4* petals. Moreover, forced expression of AN1 and PH4 is sufficient to activate *CAC16.5* in leaves (Figure 7).

Cys proteases have regulatory functions in a variety of processes. In animals, Cys proteases play an important role in programmed cell death. In plants, Cys proteases have also been implicated in programmed cell death (Elbaz et al., 2002; Kuroyanagi et al., 2005) and various aspects of defense responses (Kruger et al., 2002; Hatsugai et al., 2004; Matarasso et al., 2005). Recent data suggest that (some) Cys proteases have DNA binding activity and can be involved directly in transcriptional activation (Matarasso et al., 2005). Currently, we are investigating the function of *CAC16.5* and other *AN1*/*PH4*-controlled genes in vacuolar acidification by reverse genetic strategies.

Interaction of AN1 and PH4

Our yeast two-hybrid data indicate that AN1 can interact with the R2R3 MYB proteins AN2 and PH4 and two novel proteins that were designated MYBb1 and MYBx. Several lines of evidence indicate that these two-hybrid interactions reflect interactions that occur in vivo.

First, screening of a petal cDNA library with the N terminus of AN1 revealed interactions with only four proteins (AN2, PH4, MYBb, and MYBx) (cf. Figure 6) but not with numerous other MYBs that are expressed in petals at much higher levels (Avila et al., 1993; Mur, 1995; van Houwelingen et al., 1998). This indicates that the observed yeast two-hybrid interactions are specific. Moreover, the four interacting MYBs all seem to have a function in pigmentation. AN2 is known to regulate structural anthocyanin genes together with AN1 (Quattrocchio et al., 1993, 1998; Spelt et al., 2000) (Figure 7B), whereas PH4 regulates, together with AN1, several aspects of vacuolar physiology (acidification and fading) (de Vlaming et al., 1982, 1983; Spelt et al., 2002; this study). *MYBb1* and the closely related homolog *MYBb2* encode proteins with high similarity to AN2 and are required for the activation of anthocyanin synthesis in distinct floral tissues, whereas MYBx appears to be an inhibitor of AN1 in anthocyanin synthesis and vacuolar acidification (Kroon, 2004).

Second, in vitro synthesized PH4 and AN1 proteins form an immunoprecipitable complex, indicating that the PH4–AN1 interaction is direct.

Third, *AN1* and *PH4* mRNAs are both expressed in the epidermis of petal cells; thus, AN1–PH4 complexes have the potential to be formed there (Figure 5D). Ovaries also express *AN1* and *PH4* mRNA, but because it is unknown whether both genes are coexpressed in the same cells, it is unclear whether AN1–PH4 complexes can also form in this organ.

Fourth, in petals, anthocyanin accumulation is limited to epidermal cells, and the underlying mesophyll cells are uncolored (Koes et al., 1990; Huits et al., 1994). Hence, the flower color phenotypes of *an1*, *an2*, and *ph4* mutants result from alterations in the very same cells.

Fifth, mutations in *an1* and *ph4* affect the same target processes: vacuolar acidification, flower color fading, and the expression of *CAC16.5*. Moreover, AN1 and PH4 can induce ectopic expression of *CAC16.5*, but only when coexpressed. Because *ph2* and *ph5* mutations do not cause fading, it seems that fading is attributable to some other defect in vacuole structure or physiology occurring in both *an1* and *ph4*.

Roles of Distinct R2R3 MYB–BHLH Complexes

As shown above, our results provide evidence that AN1 activates *CAC16.5* expression and vacuolar acidification in a complex with PH4 and presumably several other unknown proteins. Ectopic expression of PH4 alone had little or no effect on the phenotype or expression of *DFR* and *CAC16.5*, but when coexpressed with high amounts of AN1, it could ectopically activate *CAC16.5* and *DFR* and caused in addition reduced vigor and more acidic leaf extracts (Figure 7; see Supplemental Figure 5 online). Because AN1 and PH4 did not induce *DFR* within the 24 h of a transient expression assay, it is possible that the induced anthocyanin synthesis in the transgenic plant is caused by an indirect effect. Alternatively, the PH4–AN1 complex might have a low affinity for anthocyanin gene promoters that becomes evident only at unphysiologically high expression levels.

Ectopic expression of the putative PH4 homologs from rice (MYB4) in heterologous systems can activate the phenylpropanoid gene *PAL* (encoding phenylalanine ammonia lyase) and other pathways that result in dwarfism and induced freezing/chilling tolerance (Vannini et al., 2004). The induction of *PAL*, however, is very moderate (less than twofold) (Vannini et al., 2004), possibly because the BHLH partner of rice MYB4 was missing or because the induction is indirect. Ectopic overexpression of the grape homolog MYB5 in tobacco enhanced the pigmentation in petals and stamens but not in other tissues (Deluc et al., 2006), possibly reflecting the dependence on the expression of an endogenous BHLH partner. Curiously, both early (*CHS*, *CHI*, and *F3H*) and late (*DFR*) anthocyanin genes were induced by MYB5 (Deluc et al., 2006). Whether this overexpression phenotype reflects the normal MYB5 function is difficult to assess from the available data.

Given that anthocyanin genes are normally expressed in *ph4* flowers, these appear to be activated through interactions with a distinct R2R3 MYB protein. Most likely, the R2R3 MYB partner required for the activation of anthocyanin genes is AN2, because (1) AN2 is known to be required for the expression of structural anthocyanin genes (Quattrocchio et al., 1993); (2), it is, in addition to PH4, one of the few MYB proteins in petals that can bind to AN1 (Figure 6; see Supplemental Figure 3 online); (3) it can functionally replace C1 of maize (Quattrocchio et al., 1998), which is known to bind directly to the promoters of structural anthocyanin genes (Sainz et al., 1997); and (4) coexpression of AN2 with AN1 or JAF13 activates *DFR* fast enough to be detected within 24 h in transient expression assays, consistent with AN2 activating *DFR* directly, like AN1 (Quattrocchio et al., 1998, 1999; Spelt et al., 2000) (Figure 6). Moreover, using GLUCOCORTICOID RECEPTOR fusions, it was shown that TT2 of *Arabidopsis* activates *DFR* directly (Baudry et al., 2004). Together, these findings suggest a model in which AN1 activates vacuolar acidification or anthocyanin synthesis by binding to PH4 or AN2, respectively.

Work in *Arabidopsis* led to very similar models, which propose that the partially redundant BHLH proteins GL3 (Payne et al., 2000), EGL3 (Bernhardt et al., 2003; Zhang et al., 2003), and TT8 (Nesi et al., 2000) activate the synthesis of anthocyanin and

proanthocyanidin pigments, the production of seed mucilage, the development of trichomes on leaves and stems, and the specification of nonhair fate (atrichoblast) in certain cells of the root epidermis through interactions with distinct R2R3 MYB proteins that are specific for each pathway (Zhang et al., 2003; Baudry et al., 2004; Pesch and Hulskamp, 2004; Zimmermann et al., 2004).

These simple models explain many of the observations, but not all of them, and therefore are likely to be incomplete and possibly even incorrect in some details.

First, these models predict that overexpression of PH4 might compete with AN2, resulting in an *an2*-like phenotype (reduced anthocyanin synthesis), whereas overexpression of AN2 might result in a *ph4*-like phenotype (blue flowers). However, such

Table 1. Description of Primers Used for PCR

Name	Gene	Sequence	Orientation
282	*AN1*	AAGAATTCATGCAGCTGCAAACCATG	F
283	*AN1*	ATCTCGAGGGACAAAGTGAGAGATC	R
284	*AN1*	TTCTCGAGCATCTCCGGCTACTCC	R
123	*AN1*	GGGAATTCTATGGTGTCACCAAG	R
126	*AN1*	TAGGATCCAGCCTTATCTGAGCACT	F
325	*JAF13*	GGCAATTGATGGCTATGGGATGCAAAG	F
292	*JAF13*	AACTCGAGGATCAGGCTTTGGGCAT	R
295	*JAF13*	TCCTCGAGATTTCCAGACTACTCGC	R
287	*AN2*	TAGAATTCATGAGTACTTCTAATGCATC;	F
288	*AN2*	GAGAATTCTTAATTGCTCCTCATGATCA	F
289	*AN2*	ATCTCGAGCTCTTCAATGGTCCCA	R
290	*AN2*	CTCTCGAGTCTGATCATGAGGAGCAAT	R
1051	*PH4*	CCTTGCTACAACATGGTGTT	R
1107	*PH4*	CACTCTCACCCAACGTAACATGC	F
972	*PH4*	GCCCCTGAACACCATGTTGTA	F
1136	*PH4*	GGCAATTGATGAGAACCCCATCATCATC	F
1137	*PH4*	GGCAATTGTTAATCAGTCACGGAATAGATC	F
1138	*PH4*	GGGCTCGAGGATCTATTCCGTGACTGATTAA	R
1139	*PH4*	GGGCTCGAGCTCTAACTGGGATTATATTGATC	R
1233	*PH4*	AAGCTTTCTCTAACTGGGATTATATTGA	R
1317	*PH4*	TTCTCTAGAGATGAGAACCCCATCATCAT	F
690	*PH4*	CGGGATCCTCTCTAACTGGGATTATATTG	R
1061	*PH4*	CGCCTCCATCGTCTCCTTGG	F
582	*PH4*	CTTCTCCTCCTTCATCTTC	F
1871	*CAC16.5*	GCCTCCTTATCCATCTCCAGCCC	F
1769	*CAC16.5*	GTAATGACATTCAAACAGCATCC	R
275	*CHSa*	CAGTGAGCACAAGACTGATC	F
604	*CHsa*	CTTGGATCCTTAAGTTTCTCGGGC	R
311	*CHIa*	ACGCTTTCGCACCGACCG	F
312	*CHIa*	GTAGATTTCTCGGTCTCCG	R
112	*F3H*	ATGACCGTGGTCACCAAGATTG	F
113	*F3H*	CTTCACATTTGTCTTCCGAG	R
97	*DFR*	ACAATGTTCACGCTACTGTTC	F
98	*DFR*	GTAGGAACATAGTACTCTGG	R
433	*AS*	ATGGTGAATGCAGTAGTTACAAC	F
434	*AS*	GGCATAGAACTAAACTCCACA	R
435	*AAT*	CATTACCAACTCCTAATCACC	F
436	*AAT*	GGCATAGAACTAAACTCCACA	R
229	*AN9*	CGGGATCCTTTGTCCCGTACTCC	R
230	*AN9*	GGGAATTCCATGGTTGTGAAAGTGCATG	F
19	*GAPDH*	GGTCGTTTGGTTGCAAGAGT	F
20	*GAPDH*	CTGGTTATTCCATTACAACTAC	R
Out1	*dTPH1*	GGGAATTCGCTCCGCCCCTG	F, R
Out12	*dTPH1*	C/TCAGCATTGACACCCCTTC	F
Out13	*dTPH1*	G/ACAGTGTAAATTTTGCGCAAA	F
Out10	*dTPH1*	CCCCTTTGCACCAAGTAGCTC	F
Out11	*dTPH1*	CGAAGGGGTGTCAATGCTG	R

Sequences are written in the 5′ to 3′ direction. Restriction sites that were added for cloning purposes are underlined. All primers were deoxyribonucleotides. The relative orientation of primers is indicated as forward (F) if the 3′ end of the primer points toward the 3′ end of the gene or, in case of *dTPH1* primers, if the sequence is identical to the *dTPH1* sequence in GenBank. Otherwise, the orientation is designated reverse (R).

cross-inhibition phenotypes were not observed in any of the *35S*:*PH4* or *35S*:*AN2* lines (Quattrocchio et al., 1998; Spelt et al., 2000; this study). Also, for *Arabidopsis* lines overexpressing TT2, PAP1, GL1, WER, or *Arabidopsis* MYB23, no cross-inhibitory effects of anthocyanin regulators on hair development, or vice versa, were reported (Szymanski and Marks, 1998; Lee and Schiefelbein, 1999, 2002; Borevitz et al., 2000; Kirik et al., 2001; Nesi et al., 2001).

Second, these simple models do not explain the small but clear effect of *AN2* on vacuolar acidification (Spelt et al., 2002). Gain-of-function experiments indicated that AN2 and TT2 might play an additional role as a higher order regulator in transcription activation of their BHLH partners, AN1 and TT8, respectively (Spelt et al., 2000; Nesi et al., 2001). This indirect effect of AN2 and TT2 on *DFR* expression is evident only in transgenic plants that constitutively express AN2 or TT2 (Spelt et al., 2000; Nesi et al., 2001), but it is apparently too slow to contribute to the induction of DFR within the <24 h of a transient expression assay (Quattrocchio et al., 1998; Spelt et al., 2000; Zimmermann et al., 2004). Thus, it is possible that AN2 affects vacuolar acidification indirectly through the activation of another regulatory gene that is distinct from *AN1* or *PH4*, because these are normally expressed in *an2* petal limbs (Figure 6) (Spelt et al., 2000).

Alternatively, it is possible that in vivo, larger complexes are formed that contain multiple R2R3 MYB and BHLH proteins, because yeast two-hybrid experiments indicated that TT2 can homodimerize (Baudry et al., 2004) and that EGL3 and GL3 as well as AN1 and JAF13 can form both homodimers and heterodimers (Zhang et al., 2003; Kroon, 2004). Thus, the in vivo interactions of AN2 and PH4 with AN1 need not be mutually exclusive. Clearly, the current genetic approaches need to be combined with biochemical analyses of protein complexes to solve this issue.

METHODS

Plant Material

The *Petunia hybrida* line R27 (*AN1, an4, AN11, PH2, PH4, HT1, hf1, hf2, rt, fl, FA*) was the parent for most transposon insertion/excision mutants. Line W138 arose by a transposon insertion in *AN1* (allele *an1-W138*) (Doodeman et al., 1984a; Spelt et al., 2000). Line W137 (*AN1-R, an11-W137*) arose among W138 progeny by a *dTPH1* insertion in *AN11* (*an11-W137*) and excision of the *dTPH1* copy from *an1-W138*, resulting in a full AN1 reversion (*AN1-R*) (Doodeman et al., 1984b; de Vetten et al., 1997). The alleles *ph2-A2414*, *ph3-V2068*, *ph4-X2052*, and *ph4-C3540* were identified among W138 progeny, whereas *ph4-V2153*, *ph4-V2166*, and *ph4-B3021* originate from W137. The alleles *ph4-V2153* and *ph4-V2166*, which were used for most functional analyses, were maintained in a full revertant *AN11* background in lines R149 (*AN1-R, AN11-R, ph4-V2153*) and R150 (*AN1-R, AN11-R, ph4-V2166*). For functional analyses of other *ph* alleles, *AN1-R* and/or *AN11-R* plants were selected from progeny of parents containing the *ph* allele in an *an1-W138* or *an11-W137* background. The allele *ph4-X2377* was identified among offspring in a Red Star–like family (background *AN1, AN11, rt, fl*) in the fields of a petunia breeder (Syngenta) (van Houwelingen et al., 1998). The lines V64 (*AN1, AN11, HF1, FL, RT, ph4-V64*), M60 (*AN1, AN11, ph4-V64, hf1, hf2, RT, fl*), V30 (*AN1, AN2, AN4, AN11, HF1, RT, PH2, PH4*), and V26 (*AN1, AN2, an4, AN11, HF1, RT, ph2, PH4*) were from the Amsterdam Petunia Collection (de Vlaming et al., 1983; Koes et al., 1986).

To introduce *an1-G621* in a background synthesizing 3RGac5G-substituted anthocyanins, several progeny plants with an *an1-W138, RT* phenotype were selected from the backcross (W138 × V30) × W138 (de Vetten et al., 1999) and subsequently crossed to line R153 (*an1-G621, hf1, rt*). Detailed information about the structure and resulting phenotypes of *an1-W138* and *an1-G621* can be found elsewhere (Spelt et al., 2000, 2002).

HPLC Analysis

Petal limb tissue was extracted for 16 h at 4°C in 70% methanol and 0.1% trifluoroacetic acid (TFA; 500 μL/100 mg tissue) and passed through a Spin-X centrifuge tube filter (0.22 μm; Corning). Samples (10 μL) were analyzed on a 3.9 × 150-mm reversed-phase Nova Pak C_{18} column (Waters) using a linear gradient from 15% acetonitrile, 0.1% TFA to 95% acetonitrile, 0.1% TFA over 45 min. Products were detected using a photodiode array detector (Waters) in the range 190 to 600 nm. The retention time of cyanidin 3-glucoside was determined by HPLC of the purified compound (Polyphenols Laboratories).

pH Assay

The pH of petal extracts was measured by grinding the petal limbs of two corollas in 6 mL of distilled water. The pH was measured directly (within 1 min) with a normal pH electrode to avoid the possibility that atmospheric CO_2 would alter the pH of the extract.

The actual pH values measured for specific plants showed some variation in time, possibly as a result of variable environmental conditions in the greenhouse, but the differences between distinct genotypes were constant. Therefore, the absolute pH values can be reliably compared between samples/genotypes that were measured within one experiment (i.e., one figure panel) but much less between distinct experiments (i.e., distinct figure panels).

DNA and RNA Methodology

Transposon display analysis of homozygous *ph4-B3021* and wild-type (*PH4*) progenitor plants was performed essentially as described (van den Broek et al., 1998), with some modifications (Tobeña-Santamaria et al., 2002). One fragment of 98 bp (containing 66 bp of *dTph1* sequence and 32 bp of flanking sequence) that matched the *ph4* genotype of the plants analyzed was cut from the gel, amplified with the same primers used to generate the displayed fragment (out 10 and the *Mse*I+C AFLP primer), cloned into a pGEM-T Easy vector (Promega), and sequenced.

A full-size *PH4* cDNA clone was isolated by screening a petal cDNA library made from the *PH4* line R27; the corresponding genomic region was amplified from R27 with primers complementary to the cDNA ends.

cDNA-AFLP analysis of RNA isolated from wild-type, *an1*, *ph3*, *ph4*, and *ph5* petal limbs was performed essentially as described (Bachem et al., 1996) using the restriction enzymes *Mse*I and *Eco*RI and corresponding adapters and primers. *CAC16.5* was identified as a 161-bp cDNA-AFLP fragment that was present in wild-type and *ph5* petals but absent in *an1*, *ph3*, and *ph4* petals. A 1169-bp *CAC.16.5* cDNA containing part of the protein-coding sequence was isolated by screening a petal cDNA library with the 161-bp fragment.

RNA isolation and RT-PCR analysis were performed as described (de Vetten et al., 1997; Quattrocchio et al., 1998). cDNA products were amplified using primers specific for *CHSa* (primers 275 and 604), *CHIa* (311 and 312), *AN3*/*F3H* (112 and 113), *DFR* (97 and 98), *AS* (433 and 434), *AAT* (435 and 436), *AN9* (229 and 230), *CAC16.5* (1871 and 1769), *PH4* (1233 and 1317), *AN1* (123 and 126), or *GAPDH* (19 and 20) and a reduced number of PCR cycles (*GAPDH* and *CAC16.5*, 18 cycles; *CHSa*, *CHIa*, *F3H*/*AN3*, *DFR*, *AS*, *AAT*, and *AN9*, 20 cycles; *AN1* and *PH4*, 24 cycles). Because the yield of PCR products was too low for detection by ethidium

bromide, they were visualized by gel blot hybridization (using ^{32}P-labeled cDNA probes) and phosphor imaging, For each gene–primer combination, we determined whether the RT-PCR response was linear and quantitative (at different numbers of PCR cycles) by assaying dilution series of cDNA samples in which transcripts were highly abundant or that had been spiked with cDNA fragments.

The 3′RACE of *PH4* was done as described previously (Frohman et al., 1988) using a *PH4*-specific primer (1136) and a primer complementary to the poly(A) tail.

RNA in situ hybridization was performed as described (Souer et al., 1996) using RNA probes obtained by in vitro transcription with T7 or SP6 RNA polymerase. The templates were generated by PCR on cDNAs cloned in plasmid vectors using a vector-specific primer that anneals just upstream of the T7 or SP6 promoter and one gene-specific primer. The *PH4* probe spanned the region encoding the C-terminal domain (generated with primer 582 and a vector-specific primer) and lacked the conserved MYB domain region. For *AN1* and *DFR*, a cDNA fragment spanning the coding sequence and the 3′ untranslated region was used. Because anthocyanins present in flowers made it difficult to detect the weak colorigenic signals for *AN1* and *PH4* mRNA unambiguously, we used petals from the *an3* lines W62 and W37.

Sequence Analysis

DNA sequences were determined as described (Spelt et al., 2002) and analyzed with the program Geneworks (Intelligenetics). Multiple sequence alignments were produced with a Web-based version of ClustalW (http://crick.genes.nig.ac.jp/homology/clustalw-e.shtml) using default settings (Matrix = blossom; GAPOPEN = 0, GAPEXT = 0, GAPDIST = 8, MAXDIV = 40). The phylogenetic tree was calculated using the neighbor-joining method and bootstrap analysis (1000 replicates) using PHYLIP via the same website and visualized with Treeviewer version 1.6.6 (http://taxonomy.zoology.gla.ac.uk/rod/rod.html).

To construct the tree shown in Figure 4A, we aligned the 104–amino acid region spanning the MYB domain (see Supplemental Figure 2 online), as defined by Stracke et al. (2001), taken from the following GenBank accession numbers: Ph PH4, AY973324; Ph AN2, AAF66727; Ph ODO1, AAV98200; Ph MYBPh1, CAA78386; Ph MYBPh2, CAA78387; Ph MYBPh3, CAA78388; Gh BNLGHi233, AAK19611; Vv MYBCS1, AAS68190, Vv MYB5, AAX51291; Sl ANT1, AAQ55181; Vv MYBA2, BAD18978; Vv MYBA1, BAD18980; Vv MYBA3, BAD18179; Os MYB4, BAA23340; Zm Pl, AAA19821; Zm C1, AAK09327. For sequences of the *Arabidopsis thaliana* MYB proteins, we used the same accessions as Stracke et al. (2001).

Yeast Two-Hybrid Analysis

To generate plasmids expressing the coding sequences of *AN1*, *AN2*, *JAF13*, and *PH4*, these were amplified by PCR from corresponding cDNA clones using a polymerase with proofreading activity (*Pfu*I) and primers that were at the 3′ end complementary to the coding sequences and that contained extra nucleotides at the 5′ end with a *Xho*I, *Eco*RI, or *Mun*I restriction site to facilitate in-frame cloning in the two hybrid vectors pBD-GAL4Cam and pAD-GAL4-2.1 (Stratagene) downstream of the GAL4^{BD} or GAL4^{AD} coding sequence. The full AN1 coding sequence was amplified with primers 282 and 283 (Table 1), and the N-terminal domain was amplified with primers 282 and 284. The corresponding regions of *JAF13* were generated with the primer pairs 325/295 and 325/292, respectively. The full coding sequence of *PH4* was generated with the primer pair 1136/1139, the MYB domain with 1136/1138, and the C-terminal domain with 1137/1139. The corresponding regions of *AN2* were amplified with primer pairs 287/289, 287/288, and 290/289, respectively. The inserts of the recombinant plasmids were sequenced to ensure that no mutations had occurred during PCR amplification.

For all experiments, we used the yeast strain PJ69 (James et al., 1996), which harbors *HIS3*, *ADE2*, and *LACz* reporter genes driven by distinct GAL4-responsive promoters.

A petunia cDNA library was generated in pAD-GAL4-2.1 from poly(A)$^+$ RNA that had been isolated from petal limbs of line R27 using the HybriZap system (Stratagene), according to the instructions of the supplier. The original library (8×10^7 primary recombinants) was amplified and used for mass excision of plasmid DNA according to the instructions. This cDNA library was screened by introducing 10-μg portions of library DNA into yeast PJ69 cells expressing the N-terminal 238 amino acids of AN1 fused to the GAL4 DNA binding domain (AN1$^{1\text{-}238}$GAL4^{BD}). Transformed cells were plated on dropout medium lacking Leu, Trp, and His. After ~1 week of growth at 30°C, the colonies that appeared were replicated on plates lacking Leu, Trp, His, and adenine and grown for another 3 d at 30°C. Plasmid DNA was isolated from positive (*HIS, ADE*) colonies, transformed in *Escherichia coli*, and sequenced. Plasmids isolated from *E. coli* were subsequently reintroduced in PJ69 yeast cells, either alone or together with the bait plasmid expressing AN1$^{1\text{-}238}$GAL4^{BD}. Only plasmids that specified a *HIS, ADE* phenotype when cotransformed with the bait vector, but not when cotransformed with the empty pAD-GAL4-2.1 vector or when transformed alone, were considered positives and analyzed further.

Transient Expression Assays and Generation of Stable Transformants

To construct the *35S*:*PH4* gene, we amplified the *PH4* coding region using primers complementary to the beginning (primer 1136) and end (primer 690) of the coding sequence that had been extended with *Xba*I and *Bam*HI restriction sites, respectively. Amplification products were cut with *Xba*I and *Bam*HI and ligated to the *Xba*I and *Bam*HI sites of the T-DNA vector pGreen 3K (Hellens et al., 2000) between the 35S promoter and the 3′ polyadenylation signal of *Cauliflower mosaic virus*. The gene construct was sequenced to ensure that no errors had occurred. The origins of *35S*:*AN1*, *35S*:*AN2*, *35S*:*JAF13*, *DFR*:*LUC*, and *35S*:*GUS* have been described elsewhere (Quattrocchio et al., 1998; Spelt et al., 2000).

Transient expression assays were performed by particle bombardment of petunia W115 leaves (genotype *AN1, an2, an4, AN11, PH4*) as described previously (de Vetten et al., 1997; Quattrocchio et al., 1998). The *an2* and *an4* mutations in W115 do not affect the expression of anthocyanin genes in tissues other than petals and anthers (Quattrocchio et al., 1993).

Transgenic plants expressing *35S*:*PH4* were obtained by *Agrobacterium tumefaciens*–mediated leaf disc transformation of the F1 hybrid V26 × R162 (genotype *ph2*). Of four transformants, one expressed the *35S*:*PH4* transgene, resulting in partial rescue of the *ph2* phenotype. This transformant was crossed to *35S*:*AN1* plants in a W242 (*an1, PH2*) background (Spelt et al., 2000) or, as a control, to nontransgenic W242 plants to obtain *35S*:*PH4* plants in a wild-type (*AN1, AN2, AN11, PH4*) and *35S*:*AN1* background. Segregation of the transgenes in these crosses was monitored by PCR, using primer combinations specific for each transgene.

Because for *an2* null mutants no isogenic wild-type (*AN2*) lines are available, we transformed an *an2* F1 hybrid (W115 × W59; genotype *AN1, an2, an4, RT,AN11, PH2, PH4*) with *35S*:*AN2* or, as a control, the empty T-DNA vector and used plants in which *35S*:*AN2* complemented the *an2* mutation for comparison with *an2* plants containing the empty vector (Quattrocchio et al., 1998).

Protein Methods

To synthesize AN1 and PH4 proteins in vitro, the full-size cDNAs were cloned in pBluescript KS+ plasmids behind the T3 polymerase promoter, and the region spanning the T3 promoter and the cDNA insert was

amplified by PCR using primers complementary to pBluescript. Amplification products were purified on a minipreparation spin column (Qiagen), extracted with phenol, and precipitated with ethanol. We used 0.5 μg of PCR fragment to program an in vitro transcription and translation system (TNT-coupled wheat germ extract) as recommended by the supplier (Promega). For the synthesis of radiolabeled proteins, wheat germ extract lacking Met was supplemented with 20 μCi of [^{35}S]Met (Amersham). For the synthesis of unlabeled AN1 protein, a 1:1 mixture of wheat germ extracts lacking either Met or Leu was used.

For (co)immunoprecipitation, translation products were mixed in a 1:1 ratio, and 1 μL of a mouse anti-AN1 serum (Spelt et al., 2002) was added and incubated for 1 h at 4°C. Subsequently, 10 μL of protein G–agarose beads (Actigen) was added and incubation was continued for 16 h at 4°C in a rotation apparatus. The agarose beads were washed twice in 10 mM Na-phosphate, pH 7.2, 150 mM NaCl, and 0.05% Tween, resuspended in SDS sample buffer, boiled for 2 min, and size-separated on a 12.5% polyacrylamide-SDS protein gel. Gels were fixed and dried, and radioactivity was detected using a phosphor imager.

Accession Numbers

Sequence data from this article have been deposited with the GenBank/EMBL data libraries under accession numbers AY187282 (*dTPH7*), AY973324 (*PH4*), and AY371317 (*CAC16.5*).

Supplemental Data

The following materials are available in the online version of this article.

Supplemental Figure 1. HPLC Analysis of Methanol-Extractable Anthocyanins and Phenylpropanoids in Petal Limbs of *PH4* and *ph4-V2153* Flowers in the R27 Genetic Background.

Supplemental Figure 2. Alignment of MYB Domains of PH4 and Other R2R3 MYB Proteins.

Supplemental Figure 3. Coimmunoprecipitation of AN1 and PH4 Synthesized in Vitro by Coupled Transcription and Translation.

Supplemental Figure 4. Alignment of the Protein Encoded by a Partial *CAC16.5* cDNA of Petunia to Cys/Thiol Proteases of Other Species.

Supplemental Figure 5. Phenotype of *35S:AN1 35S:PH4* Double Transgenic Plants.

Supplemental Table 1. Complementation Analysis of *ph2*, *ph3*, and *ph4* Mutants.

ACKNOWLEDGMENTS

We thank Pieter Hoogeveen, Martina Meesters, and Daisy Kloos for plant care and Riet Vooijs for help with the HPLC analyses. This research was supported by grants from the European Union, the Netherlands Technology Foundation, and the Netherlands Organization for Scientific Research.

Received May 11, 2005; revised March 8, 2006; accepted March 18, 2006; published April 7, 2006.

REFERENCES

Alfenito, M.R., Souer, E., Goodman, C.D., Buell, R., Mol, J., Koes, R., and Walbot, V. (1998). Functional complementation of anthocyanin sequestration in the vacuole by widely divergent glutathione *S*-transferases. Plant Cell **10,** 1135–1149.

Avila, A., Nieto, C., Cañas, L., Benito, J., and Paz-Ares, J. (1993). *Petunia hybrida* genes related to the maize regulatory *C1* gene and to the animal *myb* proto-oncogenes. Plant J. **3,** 553–562.

Bachem, C.W., van der Hoeven, R.S., de Bruijn, S.M., Vreugdenhil, D., Zabeau, M., and Visser, R.G. (1996). Visualization of differential gene expression using a novel method of RNA fingerprinting based on AFLP: Analysis of gene expression during potato tuber development. Plant J. **9,** 745–753.

Baudry, A., Heim, M.A., Dubreucq, B., Caboche, M., Weisshaar, B., and Lepiniec, L. (2004). TT2, TT8, and TTG1 synergistically specify the expression of *BANYULS* and proanthocyanidin biosynthesis in *Arabidopsis thaliana.* Plant J. **39,** 366–380.

Bernhardt, C., Lee, M.M., Gonzalez, A., Zhang, F., Lloyd, A., and Schiefelbein, J. (2003). The bHLH genes *GLABRA3* (*GL3*) and *ENHANCER OF GLABRA3* (*EGL3*) specify epidermal cell fate in the *Arabidopsis* root. Development **130,** 6431–6439.

Borevitz, J.O., Xia, Y., Blount, J., Dixon, R.A., and Lamb, C. (2000). Activation tagging identifies a conserved MYB regulator of phenylpropanoid biosynthesis. Plant Cell **12,** 2383–2394.

Brugliera, F., and Koes, R. (2001). Plant anthocyanidin rutinoside aromatic acyl transferases. International Patent Publication Number WO01/72984.

Carey, C.C., Strahle, J.T., Selinger, D.A., and Chandler, V.L. (2004). Mutations in the *pale aleurone color1* regulatory gene of the *Zea mays* anthocyanin pathway have distinct phenotypes relative to the functionally similar *TRANSPARENT TESTA GLABRA1* gene in *Arabidopsis thaliana.* Plant Cell **16,** 450–464.

Davies, S.A., Goodwin, S.F., Kelly, D.C., Wang, Z., Sozen, M.A., Kaiser, K., and Dow, J.A. (1996). Analysis and inactivation of vha55, the gene encoding the vacuolar ATPase B-subunit in *Drosophila melanogaster* reveals a larval lethal phenotype. J. Biol. Chem. **271,** 30677–30684.

Deluc, L., Barrieu, F., Marchive, C., Lauvergeat, V., Decendit, A., Richard, T., Carde, J.P., Merillon, J.M., and Hamdi, S. (2006). Characterization of a grapevine R2R3-MYB transcription factor that regulates the phenylpropanoid pathway. Plant Physiol. **140,** 499–511.

de Vetten, N., Quattrocchio, F., Mol, J., and Koes, R. (1997). The *an11* locus controlling flower pigmentation in petunia encodes a novel WD-repeat protein conserved in yeast, plants and animals. Genes Dev. **11,** 1422–1434.

de Vetten, N., ter Horst, J., van Schaik, H.-P., den Boer, B., Mol, J., and Koes, R. (1999). A cytochrome b5 is required for full activity of flavonoid 3′5′-hydroxylase, a cytochrome P450 involved in the formation of blue flower colors. Proc. Natl. Acad. Sci. USA **96,** 778–783.

de Vlaming, P., Cornu, A., Farcy, E., Gerats, A.G.M., Maizonnier, D., Wiering, H., and Wijsman, H.J.W. (1984). *Petunia hybrida*: A short description of the action of 91 genes, their origin and their map location. Plant Mol. Biol. Rep. **2,** 21–42.

de Vlaming, P., Schram, A.W., and Wiering, H. (1983). Genes affecting flower colour and pH of flower limb homogenates in *Petunia hybrida.* Theor. Appl. Genet. **66,** 271–278.

de Vlaming, P., van Eekeres, J.E.M., and Wiering, H. (1982). A gene for flower colour fading in *Petunia hybrida.* Theor. Appl. Genet. **61,** 41–46.

Doodeman, M., Boersma, E.A., Koomen, W., and Bianchi, F. (1984a). Genetic analysis of instability in *Petunia hybrida.* I. A highly unstable mutation induced by a transposable element inserted at the *An1* locus for flower colour. Theor. Appl. Genet. **67,** 345–355.

Doodeman, M., Gerats, A.G.M., Schram, A.W., de Vlaming, P., and Bianchi, F. (1984b). Genetic analysis of instability in *Petunia hybrida.* II. Unstable mutations at different loci as the result of transpositions of the genetic element inserted at the *An1* locus. Theor. Appl. Genet. **67,** 357–366.

Elbaz, M., Avni, A., and Weil, M. (2002). Constitutive caspase-like machinery executes programmed cell death in plant cells. Cell Death Differ. **9,** 726–733.

Ferea, T.L., and Bowman, B.J. (1996). The vacuolar ATPase of *Neurospora crassa* is indispensable: Inactivation of the vma-1 gene by repeat-induced point mutation. Genetics **143,** 147–154.

Ferrario, S., Busscher, J., Franken, J., Gerats, T., Vandenbussche, M., Angenent, G.C., and Immink, R.G. (2004). Ectopic expression of the petunia MADS box gene UNSHAVEN accelerates flowering and confers leaf-like characteristics to floral organs in a dominant-negative manner. Plant Cell **16,** 1490–1505.

Frohman, M.A., Dush, M.K., and Martin, G.R. (1988). Rapid production of full-length cDNAs from rare transcripts: Amplification using a single gene-specific oligonucleotide primer. Proc. Natl. Acad. Sci. USA **85,** 8998–9002.

Fukada-Tanaka, S., Inagaki, Y., Ymaguchi, T., Saito, N., and Iida, S. (2000). Colour-enhancing protein in blue petals. Nature **407,** 581.

Galway, M.E., Masucci, J.D., Lloyd, A.M., Walbot, V., Davis, R.W., and Schiefelbein, J.W. (1994). The *TTG* gene is required to specify epidermal cell fate and cell patterning in the Arabidopsis root. Dev. Biol. **166,** 740–754.

Gaxiola, R.A., Fink, G.R., and Hirschi, K.D. (2002). Genetic manipulation of vacuolar proton pumps and transporters. Plant Physiol. **129,** 967–973.

Goff, S.A., Cone, K.C., and Chandler, V.L. (1992). Functional analysis of the transcription activator encoded by the maize B-gene: Evidence for a direct functional interaction between two classes of regulatory proteins. Genes Dev. **6,** 864–875.

Goff, S.A., Cone, K.C., and Fromm, M.E. (1991). Identification of functional domains in the maize transcriptional activator C1—Comparison of wild-type and dominant inhibitor proteins. Genes Dev. **5,** 298–309.

Grotewold, E., Sainz, M.B., Tagliani, L., Hernandez, J.M., Bowen, B., and Chandler, V.L. (2000). Identification of the residues in the Myb domain of maize C1 that specify the interaction with the bHLH cofactor R. Proc. Natl. Acad. Sci. USA **97,** 13579–13584.

Hatsugai, N., Kuroyanagi, M., Yamada, K., Meshi, T., Tsuda, S., Kondo, M., Nishimura, M., and Hara-Nishimura, I. (2004). A plant vacuolar protease, VPE, mediates virus-induced hypersensitive cell death. Science **305,** 855–858.

Hellens, R.P., Edwards, E.A., Leyland, N.R., Bean, S., and Mullineaux, P.M. (2000). pGreen: A versatile and flexible binary Ti vector for Agrobacterium-mediated plant transformation. Plant Mol. Biol. **42,** 819–832.

Holton, T.A., Brugliera, F., Lester, D.R., Tanaka, Y., Hyland, G.D., Menting, J.G.T., Lu, C.-Y., Farcy, E., Stevenson, T.W., and Cornish, E.C. (1993). Cloning and expression of cytochrome P450 genes controlling flower colour. Nature **336,** 276–279.

Huits, H.S.M., Gerats, A.G.M., Kreike, M.M., Mol, J.N.M., and Koes, R.E. (1994). Genetic control of dihydroflavonol 4-reductase gene expression in *Petunia hybrida.* Plant J. **6,** 295–310.

Inoue, H., Noumi, T., Nagata, M., Murakami, H., and Kanazawa, H. (1999). Targeted disruption of the gene encoding the proteolipid subunit of mouse vacuolar H(+)-ATPase leads to early embryonic lethality. Biochim. Biophys. Acta **1413,** 130–138.

James, P., Halladay, J., and Craig, E.A. (1996). Genomic libraries and a host strain designed for highly efficient two-hybrid selection in yeast. Genetics **144,** 1425–1436.

Jiang, C., Gu, X., and Peterson, T. (2004). Identification of conserved gene structures and carboxy-terminal motifs in the Myb gene family of Arabidopsis and *Oryza sativa* L. ssp. *indica.* Genome Biol. **5,** R46.

Kirik, V., Lee, M.M., Wester, K., Herrmann, U., Zheng, Z., Oppenheimer, D., Schiefelbein, J., and Hulskamp, M. (2005). Functional diversification of MYB23 and GL1 genes in trichome morphogenesis and initiation. Development **132,** 1477–1485.

Kirik, V., Schnittger, A., Radchuk, V., Adler, K., Hulskamp, M., and Baumlein, H. (2001). Ectopic expression of the *Arabidopsis AtMYB23* gene induces differentiation of trichome cells. Dev. Biol. **235,** 366–377.

Kobayashi, S., Goto-Yamamoto, N., and Hirochika, H. (2004). Retrotransposon-induced mutations in grape skin color. Science **304,** 982.

Koes, R., Verweij, C.W., and Quattrocchio, F. (2005). Flavonoids: A colorful model for the regulation and evolution of biochemical pathways. Trends Plant Sci. **5,** 236–242.

Koes, R.E., Spelt, C.E., Reif, H.J., van den Elzen, P.J., Veltkamp, E., and Mol, J.N. (1986). Floral tissue of *Petunia hybrida* (V30) expresses only one member of the chalcone synthase multigene family. Nucleic Acids Res. **14,** 5229–5239.

Koes, R.E., Van Blokland, R., Quattrocchio, F., Van Tunen, A.J., and Mol, J.N.M. (1990). Chalcone synthase promoters in petunia are active in pigmented and unpigmented cell types. Plant Cell **2,** 379–392.

Koornneef, M. (1981). The complex syndrome of *ttg* mutants. Arabidopsis Inf. Serv. **18,** 45–61.

Kroon, A.R. (2004). Transcription Regulation of the Anthocyanin Pathway in *Petunia hybrida.* PhD dissertation (Amsterdam: Vrije Universiteit).

Kroon, J., Souer, E., de Graaff, A., Xue, Y., Mol, J., and Koes, R. (1994). Cloning and structural analysis of the anthocyanin pigmentation locus *Rt* of *Petunia hybrida*: characterization of insertion sequences in two mutant alleles. Plant J. **5,** 69–80.

Kruger, J., Thomas, C.M., Golstein, C., Dixon, M.S., Smoker, M., Tang, S., Mulder, L., and Jones, J.D. (2002). A tomato cysteine protease required for Cf-2-dependent disease resistance and suppression of autonecrosis. Science **296,** 744–747.

Kuroyanagi, M., Yamada, K., Hatsugai, N., Kondo, M., Nishimura, M., and Hara-Nishimura, I. (2005). Vacuolar processing enzyme is essential for mycotoxin-induced cell death in *Arabidopsis thaliana.* J. Biol. Chem. **280,** 32914–32920.

Lee, M.M., and Schiefelbein, J. (1999). WEREWOLF, a MYB-related protein in Arabidopsis, is a position-dependent regulator of epidermal cell patterning. Cell **99,** 473–483.

Lee, M.M., and Schiefelbein, J. (2001). Developmentally distinct MYB genes encode functionally equivalent proteins in Arabidopsis. Development **128,** 1539–1546.

Lee, M.M., and Schiefelbein, J. (2002). Cell pattern in the Arabidopsis root epidermis determined by lateral inhibition with feedback. Plant Cell **14,** 611–618.

Li, S.F., Santini, J.M., Nicolaou, O., and Parish, R.W. (1996). A novel myb-related gene from *Arabidopsis thaliana.* FEBS Lett. **379,** 117–121.

Lloyd, A.M., Walbot, V., and Davis, R.W. (1992). *Arabidopsis* and *Nicotiana* anthocyanin production activated by maize regulators *R* and *C1.* Science **258,** 1773–1775.

Maeshima, M. (2001). Tonoplast transporters: Organization and function. Annu. Rev. Plant Physiol. Plant Mol. Biol. **52,** 469–497.

Matarasso, N., Schuster, S., and Avni, A. (2005). A novel plant cysteine protease has a dual function as a regulator of 1-aminocyclopropane-1-carboxylic acid synthase gene expression. Plant Cell **17,** 1205–1216.

Mathews, H., Clendennen, S.K., Caldwell, C.G., Liu, X.L., Connors, K., Matheis, N., Schuster, D.K., Menasco, D.J., Wagoner, W., Lightner, J., and Wagner, D.R. (2003). Activation tagging in tomato identifies a transcriptional regulator of anthocyanin biosynthesis, modification, and transport. Plant Cell **15,** 1689–1703.

Mur, L. (1995). Characterization of Members of the *myb* Gene Family of Transcription Factors from *Petunia hybrida.* PhD dissertation (Amsterdam: Vrije Universiteit).

Nesi, N., Debeaujon, I., Jond, C., Pelletier, G., Caboche, M., and Lepiniec, L. (2000). The *TT8* gene encodes a basic helix-loop-helix

domain protein required for expression of DFR and BAN genes in Arabidopsis siliques. Plant Cell **12,** 1863–1878.

Nesi, N., Jond, C., Debeaujon, I., Caboche, M., and Lepiniec, L. (2001). The Arabidopsis *TT2* gene encodes an R2R3 MYB domain protein that acts as a key determinant for proanthocyanidin accumulation in developing seed. Plant Cell **13,** 2099–2114.

Oka, T., and Futai, M. (2000). Requirement of V-ATPase for ovulation and embryogenesis in *Caenorhabditis elegans.* J. Biol. Chem. **275,** 29556–29561.

Oppenheimer, D.G., Herman, P.L., Sivakumaran, S., Esch, J., and Marks, M.D. (1991). A *myb* gene required for leaf trichome differentiation in *Arabidopsis* is expressed in stipules. Cell **67,** 483–493.

Payne, C.T., Zhang, F., and Lloyd, A.M. (2000). *GL3* encodes a bHLH protein that regulates trichome development in Arabidopsis through interaction with GL1 and TTG1. Genetics **156,** 1349–1362.

Pesch, M., and Hulskamp, M. (2004). Creating a two-dimensional pattern *de novo* during *Arabidopsis* trichome and root hair initiation. Curr. Opin. Genet. Dev. **14,** 422–427.

Quattrocchio, F., Wing, J.F., Leppen, H.T.C., Mol, J.N.M., and Koes, R.E. (1993). Regulatory genes controlling anthocyanin pigmentation are functionally conserved among plant species and have distinct sets of target genes. Plant Cell **5,** 1497–1512.

Quattrocchio, F., Wing, J.F., van der Woude, K., Mol, J.N.M., and Koes, R. (1998). Analysis of bHLH and MYB-domain proteins: Species-specific regulatory differences are caused by divergent evolution of target anthocyanin genes. Plant J. **13,** 475–488.

Quattrocchio, F., Wing, J., van der Woude, K., Souer, E., de Vetten, N., Mol, J., and Koes, R. (1999). Molecular analysis of the *anthocyanin2* gene of *Petunia* and its role in the evolution of flower color. Plant Cell **11,** 1433–1444.

Ramsay, N.A., Walker, A.R., Mooney, M., and Gray, J.C. (2003). Two basic-helix-loop-helix genes (MYC-146 and GL3) from Arabidopsis can activate anthocyanin biosynthesis in a white-flowered *Matthiola incana* mutant. Plant Mol. Biol. **52,** 679–688.

Sainz, M., Grotewold, E., and Chandler, V. (1997). Evidence for direct activation on an anthocyanin promoter by the maize C1 protein and comparison of DNA binding by related Myb-domain proteins. Plant Cell **9,** 611–625.

Schumacher, K., Vafeados, D., McCarthy, M., Sze, H., Wilkins, T., and Chory, J. (1999). The *Arabidopsis det3* mutant reveals a central role for the vacuolar H^+-ATPase in plant growth and development. Genes Dev. **13,** 3259–3270.

Shirley, B.W., Kubasek, W.L., Storz, G., Bruggemann, E., Koornneef, M., Ausubel, F.M., and Goodman, H.M. (1995). Analysis of Arabidopsis mutants deficient in flavonoid biosynthesis. Plant J. **8,** 659–671.

Singh, S., Tang, H.K., Lee, J.Y., and Saunders, G.F. (1998). Truncation mutations in the transactivation region of PAX6 result in dominant-negative mutants. J. Biol. Chem. **273,** 21531–21541.

Souer, E., van Houwelingen, A., Kloos, D., Mol, J.N.M., and Koes, R. (1996). The *no apical meristem* gene of petunia is required for pattern formation in embryos and flowers and is expressed at meristem and primordia boundaries. Cell **85,** 159–170.

Spelt, C., Quattrocchio, F., Mol, J., and Koes, R. (2000). *anthocyanin1* of petunia encodes a basic helix-loop-helix protein that directly activates structural anthocyanin genes. Plant Cell **12,** 1619–1631.

Spelt, C., Quattrocchio, F., Mol, J., and Koes, R. (2002). *ANTHOCYANIN1* of petunia controls pigment synthesis, vacuolar pH, and seed coat development by genetically distinct mechanisms. Plant Cell **14,** 2121–2135.

Stracke, R., Werber, M., and Weisshaar, B. (2001). The R2R3-MYB gene family in *Arabidopsis thaliana.* Curr. Opin. Plant Biol. **4,** 447–456.

Strompen, G., Dettmer, J., Stierhof, Y.D., Schumacher, K., Jurgens, G., and Mayer, U. (2005). Arabidopsis vacuolar H-ATPase subunit E isoform 1 is required for Golgi organization and vacuole function in embryogenesis. Plant J. **41,** 125–132.

Szponarski, W., Sommerer, N., Boyer, J.C., Rossignol, M., and Gibrat, R. (2004). Large-scale characterization of integral proteins from Arabidopsis vacuolar membrane by two-dimensional liquid chromatography. Proteomics **4,** 397–406.

Szymanski, D.B., and Marks, M.D. (1998). GLABROUS1 overexpression and TRIPTYCHON alter the cell cycle and trichome cell fate in Arabidopsis. Plant Cell **10,** 2047–2062.

Taiz, L. (1992). The plant vacuole. J. Exp. Biol. **172,** 113–122.

Tobeña-Santamaria, R., Bliek, M., Ljung, K., Sandberg, G., Mol, J., Souer, E., and Koes, R. (2002). FLOOZY of petunia is a flavin monooxygenase-like protein required for the specification of leaf and flower architecture. Genes Dev. **6,** 753–763.

van den Broek, D., Maes, T., Sauer, M., Zethof, J., De Keukelaire, P., D'Hauw, M., Van Montagu, M., and Gerats, T. (1998). Transposon display identifies individual transposable elements in high copy number lines. Plant J. **13,** 121–129.

Vandenbussche, M., Zethof, J., Souer, E., Koes, R., Tornielli, G.B., Pezzotti, M., Ferrario, S., Angenent, G.C., and Gerats, T. (2003). Toward the analysis of the petunia MADS box gene family by reverse and forward transposon insertion mutagenesis approaches: B, C, and D floral organ identity functions require SEPALLATA-like MADS box genes in petunia. Plant Cell **15,** 2680–2693.

van Houwelingen, A., Souer, E., Spelt, C., Kloos, D., Mol, J., and Koes, R. (1998). Analysis of flower pigmentation mutants generated by random transposon mutagenesis in *Petunia hybrida.* Plant J. **13,** 39–50.

Vannini, C., Locatelli, F., Bracale, M., Magnani, E., Marsoni, M., Osnato, M., Mattana, M., Baldoni, E., and Coraggio, I. (2004). Overexpression of the rice *Osmyb4* gene increases chilling and freezing tolerance of *Arabidopsis thaliana* plants. Plant J. **37,** 115–127.

Verdonk, J.C., Haring, M.A., van Tunen, A.J., and Schuurink, R.C. (2005). ODORANT1 regulates fragrance biosynthesis in petunia flowers. Plant Cell **17,** 1612–1624.

Walker, A.R., Davison, P.A., Bolognesi-Winfield, A.C., James, C.M., Srinivasan, N., Blundell, T.L., Esch, J.J., Marks, M.D., and Gray, J.C. (1999). The *TRANSPARENT TESTA GLABRA1* locus, which regulates trichome differentiation and anthocyanin biosynthesis in Arabidopsis, encodes a WD40 repeat protein. Plant Cell **11,** 1337–1350.

Weiss, D., Van der Luit, A.H., Kroon, J.T.M., Mol, J.N.M., and Kooter, J.M. (1993). The petunia homologue of the *Antirrhinum majus* candi and *Zea mays* A2 flavonoid genes: Homology to flavanone 3-hydroxylase and ethylene-forming enzyme. Plant Mol. Biol. **22,** 893–897.

Wiering, H. (1974). Genetics of flower colour in *Petunia hybrida* Hort. Genen Phaenen **17,** 117–134.

Wiering, H., and de Vlaming, P. (1984). Genetics of flower and pollen colors. In Monographs on Theoretical and Applied Genetics 9: Petunia, K.C. Sink, ed (Berlin: Springer-Verlag), pp. 49–67.

Winkel-Shirley, B. (2001). Flavonoid biosynthesis. A colorful model for genetics, biochemistry, cell biology, and biotechnology. Plant Physiol. **126,** 485–493.

Yoshida, K., Kondo, T., Okazaki, Y., and Katou, K. (1995). Cause of blue petal colour. Nature **373,** 291.

Yoshida, K., Toyama-Kato, Y., Kameda, K., and Kondo, T. (2003). Sepal color variation of *Hydrangea macrophylla* and vacuolar pH measured with a proton-selective microelectrode. Plant Cell Physiol. **44,** 262–268.

Zhang, F., Gonzalez, A., Zhao, M., Payne, C.T., and Lloyd, A. (2003). A network of redundant bHLH proteins functions in all TTG1-dependent pathways of *Arabidopsis.* Development **130,** 4859–4869.

Zimmermann, I.M., Heim, M.A., Weisshaar, B., and Uhrig, J.F. (2004). Comprehensive identification of *Arabidopsis thaliana* MYB transcription factors interacting with R/B-like BHLH proteins. Plant J. **40,** 22–34.